AD NUMBER

AD865808

NEW LIMITATION CHANGE

TO

Approved for public release, distribution unlimited

FROM

Distribution authorized to U.S. Gov't. agencies and their contractors; Administrative/Operational Use; Jan 1970. Other requests shall be referred to Air Force Materials Lab., MANP, Wright-Patterson AFB, OH 45433.

AUTHORITY

AFML ltr, 7 Dec 1972

AFML-TR-69-342

POLYMER STRUCTURES AND PROPERTIES

G. C. Berry, J. S. Burke, E. F. Casassa, S. M. Liwak

Carnegie-Mellon University

TECHNICAL REPORT AFML-TR-69-342

January 1970

Air Force Materials Laboratory
Air Force Systems Command
Wright-Patterson Air Force Base, Ohio

NOTICE

When government drawings, specifications, or other data are used for any purpose other than in connection with a definitely related Government procurement operation, the United States Government thereby incurs no responsibility nor any obligation whatsoever; and the fact that the Government may have formulated, furnished, or in any way supplied the said drawings, specifications, or other data, is not to be regarded by implication or otherwise as in any manner licensing the holder or any other person or corporation, or conveying any rights or permission to manufacture, use, or sell any patented invention that may in any way be related thereto.

This document is subject to special export controls and each transmittal to foreign governments or foreign nationals may be made only with prior approval of the Nonmetallic Materials Division (MANP), Air Force Materials Laboratory, Wright-Patterson Air Force Base, Ohio 45433.

The distribution of this document is limited.

Copies of this report should not be returned unless return is required by security considerations, contractual obligations, or notice on a specific document.

AFML-TR-69-342

POLYMER STRUCTURES AND PROPERTIES

G. C. Berry, J. S. Burke, E. F. Casassa, S. M. Liwak

Carnegie-Mellon University

TECHNICAL REPORT AFML-TR-69-342

January 1970

Air Force Materials Laboratory
Air Force Systems Command
Wright-Patterson Air Force Base, Ohio

FOREWORD

This report was prepared at Mellon Institute, Carnegie-Mellon University, 4400 Fifth Avenue, Pittsburgh, Pennsylvania 15213, under AF contract No. F33615-69-C-1268. The contract was initiated under Project No. 7340, "Nonmetallic and Composite Materials," Task No. 734004, "New Organic and Inorganic Polymers." It was administered under the direction of the Air Force Materials Laboratory; Dr. Matatiahu T. Gehatia, MANP, was the project engineer.

This report covers work conducted from 1 January 1969 to 31 December 1969. The report was released by the authors December 1969.

Various aspects of the investigations described herein were aided by the contributions of a number of people in addition to the listed authors. Consultations with Dr. D. J. Plazek of the University of Pittsburgh, Pittsburgh, Pennsylvania, greatly accelerated the design of the cone and plate viscometer. The freezing temperature studies were carried out by Mr. P. R. Eisaman of the Physical Services Section, Mellon Institute. The polymer utilized in the studies reported in Section V was supplied by Dr. J. K. Stille of the University of Iowa, Iowa City, Iowa.

This technical report has been reviewed and is approved.

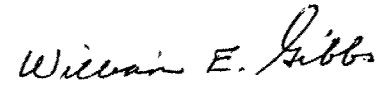

WILLIAM E. GIBBS
Chief, Polymer Branch
Nonmetallic Materials Division
Air Force Materials Laboratory

ABSTRACT

Experimental studies on the heterocyclic polymer BBB, obtained by the condensation reaction of 3,3'diaminobenzidine with naphthalene-1,4,5,8-tetracarboxylic acid, are described. Fractionations based on exclusion chromatography and selective solubility are discussed. Dilute solution properties of these fractions including light scattering and viscometry are presented.

The viscosity of concentrated solutions of the fractions in methane sulfonic acid is studied as a function of concentration and molecular weight of the polymer, and temperature. It is concluded that the solutions have a high entanglement density, even at relatively low polymer concentration, and that the segmental friction factor increases very fast with increasing polymer concentration. The latter effect is probably associated with the inability to form homogeneous solutions of BBB at high concentration.

Freezing temperature studies on solutions of a model compound of the BBB repeat unit are described. These show the compound to be diprotonated in sulphuric acid.

The design of a cone and plate viscometer for rheological studies on BBB solutions is discussed.

Dilute solution properties on a candidate 'rod-like' polymer are presented. These show that the anticipated rod-like character of the polymer is only imperfectly realized.

TABLE OF CONTENTS

THERMALLY STABLE POLYMERS

TABLE OF CONTENTS - continued

THERMALLY STABLE POLYMERS - continued

LIST OF ILLUSTRATIONS

LIST OF ILLUSTRATIONS

LIST OF TABLES

THERMALLY STABLE POLYMERS

I. Dilute Solution Studies on BBB —— G. C. Berry and E. F. Casassa

A. Introduction

Dilute solution studies have centered around the preparation and characterization of fractions of BBB with enough polymer to permit studies on concentrated solutions and on the bulk polymer. Two fractionations of this type have been completed, and light scattering and dilute solution viscometry are reported on these materials. Some heretofore unsuspected difficulties encountered in using methane sulfonic acid as a solvent for dilute solution studies are explored and correlations among the dilute solution parameters is discussed.

B. Fractionation of BBB

Two series of fractions have been prepared, one from BBB-51165 and the other from BBB-51160. Series BBB-51165-II, or simply BBB-II, was prepared by exclusion chromatography, whereas, series BBB-51160-III was prepared by successive fractional precipitation from alkaline solution.

For series BBB-II, the eluents from about sixty separate sample injections on the preparative scale porous silica column[1] were each collected in seventy parts. Independent estimates of the molecular weight distribution present in these fractions obtained by porous silica exclusion chromatography on the analytical column[1] was used to allow recombination of the seventy fractions from each injection to give a total of twelve fractions. Successive eluents from the sixty separate sample injections were then added to these twelve fractions. Series BBB-II fractions do not have as narrow a molecular weight distribution as the series BBB-51165-I fractions used in previous studies[1] since the BBB-II fractions were not refractionated to produce secondary fractions as was the case with series BBB-I. The series II fractionation was intended to provide quantities of polymer large enough for studies in concentrated solutions.

The fractionation was effected from solutions in 96 percent sulphuric acid. Each injection was 20 cc of a solution with 1.5 g/dℓ of polymer. The polymer was precipitated and washed exhaustively with deionized water. The coagulated polymer was allowed to settle from 4ℓ of water for the first few rinses. The clear supernatant water was siphoned off after the polymer settled. This procedure

became inefficient or impossible as the concentration of the electrolyte was reduced toward zero; however, since the rate of settling was either very long or the polymer did not settle at all. Consequently, it was necessary to revert to centrifugation in a Serval Model RC-60 centrifuge as the neutral point was reached. All fractions were dried in vacuum at 100°C after the final washing. Fractions ranged in size from 0.2 g to 1.8 g, with a total of 12 g recovered in series II. Weight fractions of the recovered material are given in Table I.

Series III was fractionated from an alkaline solvent system described in a previous report.[2] It was reported that BBB can be completely dissolved in 7.4 M NH_4OH to which 1.0 M KOH is added. A solution of this composition was prepared with 0.2 g/ℓ of BBB-51160. The fractions were precipitated at 30°C by successive addition of KOH until a total concentration of 10 M KOH was achieved after ten fractions had been recovered. For each cut, KOH was added to a cloud point, the solution was warmed until clear and cooled slowly to precipitate the fraction. The final fraction was recovered by sixfold dilution with water and neutralization with acetic acid. The fractions were washed with water, reprecipitated from sulphuric acid and washed exhaustively with deionized water. Weight fractions of the recovered material are given in Table I.

An unexpected phenomenon was observed during the treatment of the precipitated fractions. It was noticed that sulphuric acid solutions of the precipitated polymer were not the usual reddish-purple color, but instead were brown in hue. Spectroscopic measurements confirmed this qualitative observation, and showed that the electronic spectra of the solution very slowly changed to the usual spectra. An example of the unusual spectra is given in Figure 1. The rate of change of the absorption spectra is very slow, at 520 nm. The spectra never completely changed to that usually observed over the time period studied although the data after one week were close to the expected spectra, cf. Figure 1. On the other hand, some of the polymer with the "anomalous" spectra was recovered by precipitation in water, washed and dried. Spectra taken on this polymer, dissolved in sulphuric acid, were not unusual. The cause of this behavior is not known for certain, but it probably represents the slow oxidation of the form of BBB found in the strong alkaline solution. There is no spectroscopic evidence from either the electronic spectra on sulphuric acid solutions or the infrared spectra on the bulk polymer that the polymer reprecipitated from sulphuric acid is atypical of BBB.

C. Dilute Solution Properties

1. Solutions in Methane Sulfonic Acid

a. Preparation of Methane Sulfonic Acid. Light scattering and solution viscosity measurements have been made on dilute solutions

TABLE I

Fractionation Data on Series II and III

Fraction Number	Weight Fraction	Fraction Number	Weight Fraction
II-1	0.018	III-1	0.275
II-2	0.053	III-2	0.099
II-3	0.097	III-3	0.073
II-4	0.138	III-4	0.019
II-5	0.110	III-5	0.151
II-6	0.123	III-6	0.131
II-7	0.149	III-7	0.150
II-8	0.086	III-8	0.053
II-9	0.071	III-9	0.015
II-10	0.058	III-10	0.015
II-11	0.067	III-11	0.015
II-12	0.024		

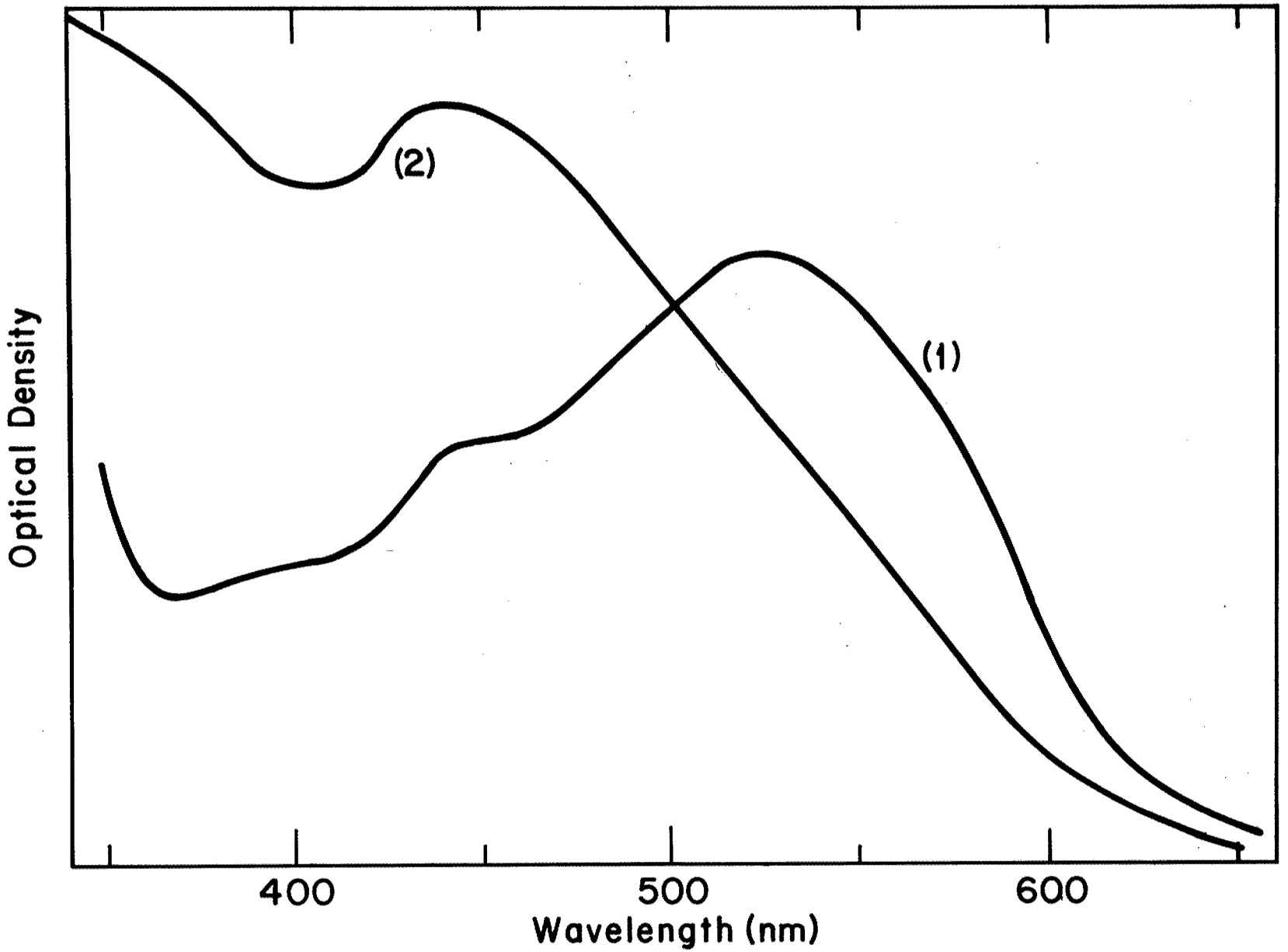

Figure 1. Electron adsorption spectra of BBB in sulphonic acid: 1) polymer treated in strong base and then dissolved in 96 per cent sulphuric acid, 2) base treated polymer after precipitation from sulphuric acid with excess water

of the series II and III fractions in methane sulfonic acid (MSA). An effort has been made to standardize the purity of the MSA used since anomalous unreproducible dilute solution viscosity data were obtained in solutions on unpurified MSA, and the intensity of light scattered from unpurified MSA solvent was found to be large and variable. The spurious results were accompanied by a strong absorption band at 282 nm for the MSA solvent. The intensity of this band was variable from sample to sample, and sometimes increased with time for a particular sample.

The first attempt to purify the sample was a vacuum distillation with an 18 inch Vigreaux column. A white solid was observed to build up at the top of the column during the initial phases of the distillation. This product was gradually washed over, but did not appear to be completely soluble in the liquid distillate. Mass spectroscopy on a sample of the white solid showed its molecular weight to be 174, which is identical to that of methane sulfonic acid anhydride:

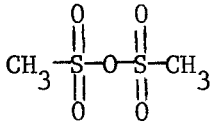

Available vapor pressure data confirm that this anhydride would have a higher vapor pressure than MSA, despite its higher molecular weight. The initial, liquid distillate did have a strong absorption band at 282 nm, but a melted sample of the suspected white methane sulfonic acid anhydride did not exhibit an identical absorption band. The 282 nm absorption was found to be present in a sample of a middle cut of MSA intentionally contaminated with a portion of the white solid; the 282 nm absorption was low for the middle cut alone. The inference is that the anhydride is protonated in MSA to produce the 282 nm absorption band. The viscosity of the initial liquid distillate with a strong 282 nm absorption band was lower by a factor of nearly 2 than that of the middle fraction, and the intensity of the scattered light was found to be very large for the initial liquid distillate. The residue from the still pot was deeply colored with dispersed black particles, but did not exhibit a pronounced absorption band at 282 nm; rather, the absorption increased slowly with decreasing wavelength from the visible region.

The second attempt to purify the MSA was a vacuum distillation with a four foot column packed with glass helices. The distillation temperature was higher in this case than in the above owing to the larger pressure drop across the packed column. The distillate from this still was found to have an appreciable absorption band at 282 nm. This band increased tenfold in samples collected after prolonged periods of total reflux. In no case was the absorption band reduced to the low levels achieved with the 18 inch column.

A batch of MSA with a strong absorption at 282 nm was sealed in a tube under vacuum and held at 100°C for four hours. The band at 282 nm was absent after this treatment, but the acid was very slightly yellowed.

It appears that at least part of the anomalous behavior of MSA may be caused by excessive concentration of the methane sulfonic acid anhydride. The equilibrium constant for the dimerization:

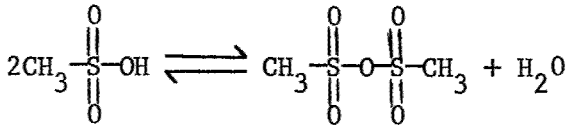

is unknown to us, but it is possible that the limited solubility of the anhydride and perhaps hydration of MSA by the water produced in the dimerization can effectively force the reaction toward the anhydride under some conditions. Elevated temperatures appear to force the reaction toward the acid, whereas prolonged storage in a dry environment appears to allow the anhydride concentration to build up. At the present time, MSA being used for dilute solutions studies has been distilled by vacuum distillation on an 18 inch column. Unfortunately, not all of the data obtained in the past has been obtained with MSA prepared in this way, cf. seq.

b. Intrinsic Viscosity Measurements. Intrinsic viscosity measurements have been made on the series II and III fractions; some data were reported earlier on the series I fractions. These results are given in Table II. As mentioned above, considerable difficulty was experienced in obtaining reproducible data on $[\eta]$ in MSA solutions. The source of this difficulty has not been definitely established, but the effects are not negligible; deviations of a factor two have been observed in some cases. The effect of water per se does not seem large enough to account for the observed deviations. For example, a sample of BBB-51165 in MSA plus 3 percent water had an intrinsic viscosity 9 percent less than the value in dry MSA. The unexpected values of $[\eta]$ are often accompanied by plots of η_{sp}/c that exhibit near zero slope over the interval $1.1 < \eta_{rel} < 1.8$, e.g., $k' \sim 0$. Data with this characteristic have been rejected systematically. The value of k' varied between 1/3 and 1/2 for the data given in Table II.

It seems probable at the present time that some of the remaining deviations among values of $[\eta]$ are related to the actual composition of the MSA used. It was suggested above that MSA is actually a mixed solvent since the acid is in equilibrium with its anhydride. Thus, the solvent flow time decreases with increasing time from the time of distillation, and the 282 nm absorption band increases with time. Comparison of $[\eta]$ values in Table II suggests

TABLE II

Intrinsic Viscosity of BBB Fractions in Methane Sulfonic Acid (t = 25°C)

Fraction	Solvent*	[η]	Fraction	Solvent*	[η]	Fraction	Solvent*	[η]
I-3	001	5.48	II-1	003	4.00	III-1	003	2.76
I-5	001	4.09	II-2	002	4.14	III-2	003	2.39
			II-2	001KR	4.17	III-2	001KR	2.57
			II-2	TECH	5.19			
I-9	001	3.63	II-3	002	3.40	III-3	003	2.12
			II-3	001KR	3.34	III-3	004	2.28
I-11	001	2.87	II-4	002	3.04	III-4	003	1.77
			II-4	001KR	2.80			
I-14	001	2.54	II-5	003	2.22	III-5	003	1.48
			II-5	TECH	3.85	III-5	003	1.41
						III-5	001KR	1.73
I-16	001	2.19	II-6	002	2.07	III-6	003	1.30
			II-6	TECH	2.73			
I-18	001	2.01	II-7	002	1.89	III-7	003	0.88
I-18	001	1.92	II-7	002	1.85			
			II-7	001KR	1.63			
			II-8	002	1.76	III-8	003	0.63
			II-9	002	1.68			
			II-10	002	1.66			
			II-10	002	1.73			

*TECH is untreated solvent. The remainder refer to distilled solvent batches, with storage under nitrogen.

that [η] decreases with the various solvents according to the ranking

$$\text{TECH} > 002 \gtrapprox 001\text{KR} > 003 \approx 004$$

Here TECH is an untreated solvent, whereas the remainder refer to batches of vacuum distilled solvent. No direct correlation between this ranking and the solvent viscosity (which is believed to reflect the anhydride concentration) was found, although the viscosity for the TECH solvent was about 7 percent less than that of the distilled solvents. Where checks have been made, the agreement between separate determinations of [η] in a single solvent appear to be much better than separate determinations in separate solvent batches (cf. II-7 and III-5). The disparity in the existing data can probably be removed by suitable normalizations to a common base. Thus, determinations of [η] for a fraction of each of the series I, II and III polymers in a single solvent should provide enough data to allow normalization of all of the existing values of [η] to a common base.

c. Light Scattering Measurements. Light scattering studies of BBB in MSA have revealed a contribution to the total observed intensity heretofore neglected. Even though the 6328 Å laser radiation is far out on the tail of the absorption band centered at 515 nm, there is sufficient fluorescence to make a contribution comparable to the intensity of scattered light. Emission spectra obtained with an Aminco-Bowman spectrofluorometer are shown in Figure 2. No emission spectra could be obtained with this instrument with an absorption wavelength of 6328 Å, testifying to the weakness of the emission. The emission would be expected to have the same spectra as that seen with the absorption wavelength at 520 nm, however. The shape of the curve shown in Figure 2 cannot be taken as authentic for the emission spectra since the Aminco-Bowman spectrofluorometer is not balanced to account for the wavelength dependence of the photomultiplier. In addition, the source intensity varies with wavelength, so the emission intensities observed with different absorption wavelengths must also be corrected for this effect. Despite these effects, however, it seems certain that there are at least three, and possibly four, separate contributions to the emission spectra; and that at least one of these could contribute to the intensity observed on irradiation with 6328 Å light. We remark that a detailed analysis of the emission spectra is likely to be very involved for a heterocyclic species such as BBB.[3] However, the observation reported below that the fluorescent intensity is independent of concentration is encouraging evidence that no appreciable intermolecular complex is formed at the concentration used for light scattering studies since such interaction almost always affects fluorescence markedly.

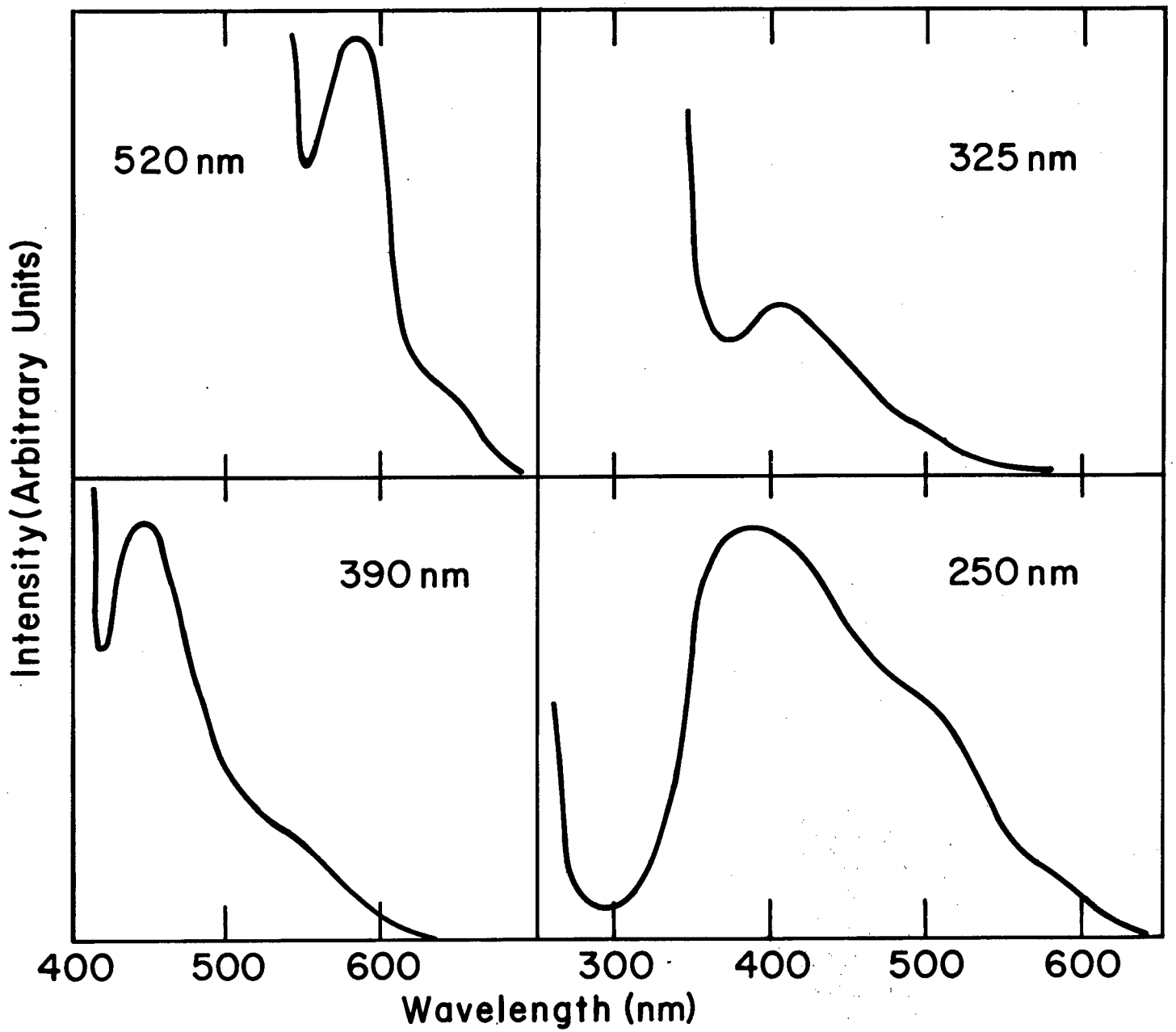

Figure 2. Fluorescence emission at the indicated excitation wavelength for solutions of BBBIII-3 in methane sulfonic acid (C ~ 2.5×10^{-5} g/cc)

The corrections to the observed intensity for a system with both absorption and fluorescence can be made as follows. We assume vertically polarized incident light with wavelength 6328 Å, and no analyzer. Let

U^V = observed intensity (a function of the scattering angle θ)

U^V_{F1} = observed fluorescence (a function of θ)

U^V_o = observed solvent scatter (a function of θ)

OD^{ℓ}_{xs} = observed excess optical density at 6328 Å for cell with pathlength ℓ.

Then the observed scattering corrected for fluorescence and absorption with a cell of diameter ℓ is equal to

$$(U^V - U^V_{F1})\alpha^{-1}$$

where

$$\alpha^{-1} = \exp(0.2303\ \ell\ OD^{10}_{xs}) \tag{1}$$

The excess Rayleigh Ratio R is then given by

$$R = k\ \sin\theta[\alpha^{-1}(U^V - U^V_{F1}) - U^V_o] \tag{2}$$

where k is a constant. The fluorescent intensity U^V_{F1} can be measured directly by comparison of the observed intensities with and without a 6328 Å band pass filter between the scattering cell and the photomultiplier. These data can then be analyzed to obtain the average value of $\sin\theta\ U^V_{F1}$, which should be independent of the scattering angle θ. We remark that this indirect method is used to obtain $U^V - U^V_{F1}$ rather than the direct single measurement with the 6328 Å band pass filter since about one-half the intensity is lost with the filter. This loss is compensated for in the present method by the averaging possible for $\sin\theta\ U^V_{F1}$, because the latter is independent of θ; comparable averaging cannot be carried out on $(U^V - U^V_{F1})\sin\theta$ itself.

It has been found empirically that U_{F1}^{v} can be correlated with the solute concentration, or equivalently, OD_{xs}^{10} by the relation

$$\frac{\sin \theta \; U_{F1}^{v}}{\alpha_F \; OD_{xs}^{10}} = K_{F1} \tag{3}$$

with

$$\alpha_F^{-1} = \exp(0.2303 \; \ell \; OD_{xs}^{10}/2) \tag{4}$$

The factor of 2 in the exponential presumably arises because the incident radiation is absorbed, whereas the emitted radiation with wavelength greater than 6328 Å is weakly absorbed. The optical density OD_{xs}^{10} can be measured precisely at 6328 Å by using the light scattering instrument itself. The scattering from the glass standard with and without an absorption cell placed in the incident beam gives the required data.

Inclusion of Eqs. (1), (3), and (4) in Eq. (2) yields the expression

$$R = k \left\{ \sin \theta \; U^{v} \exp(k_1 q) - K_{F1} q \exp(k_1 q/2) - \sin \theta \; U_o^{v} \right\} \tag{5}$$

where

$$k_1 = 0.2303 \; \ell$$

$$q = OD_{xs}^{10}$$

Differentiation with respect to q gives the error associated with an uncertainty in q:

$$\frac{\partial \ln R}{\partial q} = \frac{k_1 - \nu \exp(-k_1 q/2)[1 + k_1 q/2]}{1 - \nu q \exp(-k_1 q/2) - p \exp(-k_1 q)} \tag{6}$$

with

$$\nu = K_{F1}/\sin\,\theta\; U^{V}$$

and

$$p = U_o^{V}/U^{V}$$

For typical BBB solution, $k_1 = 3$, $\nu = 3$, and $p = 0.10$. Use of these values and an assumed uncertainty 0.02 for OD_{XS}^{1O} gives uncertainties in $\Delta R/R$ that increase from -0.4 to 8 percent as q increases from 0.2 to 1.0. These are regarded as realistic estimates of the uncertainties in the C/R values obtained from the light scattering data on BBB solutions.

A second possible difficulty in the interpretation of the data on these absorbing systems is the effect of the complex refractive index m of the solute on the scattering behavior. If we represent m by

$$m = n - in' \tag{7}$$

then the refractive index increment that should be used to analyze light scattering data for a weakly absorbing system is

$$\frac{|m - n_o|^2}{c^2} \tag{8}$$

instead of

$$\frac{(n - n_o)^2}{c^2} \tag{9}$$

as is usually used. Other than this effect, the scattering would not be expected to be much affected by the absorption unless n' is very large or the scatterer is dense and large compared to λ.[4] Insertion of the expression for m in Eq. (8) yields

$$\frac{|m - n_o|^2}{c^2} = \frac{(n - n_o)^2}{c^2} - \frac{n'^2}{c^2} \tag{10}$$

The imaginary part n' of m is related to the extinction coefficient for absorption ϵ by[4]

$$\exp(-\epsilon c \ell) = \exp\left[\frac{(-4\pi n')\ell}{\lambda}\right] \tag{11}$$

Thus

$$\frac{|m - n_o|^2}{c^2} = \frac{(n - n_o)^2}{c^2} - \left(\frac{\epsilon\lambda}{4\pi}\right)^2 \tag{12}$$

The value for ϵ for BBB solution at 6328 Å is

$$E = \frac{2.303\ OD_{xs}^{10}}{c} = 2.77 \times 10^3 \text{ cc/g cm}$$

Insertion into the above shows that the term $(\epsilon\lambda/4\pi)^2$ is only 2×10^{-4}, or negligibly small compared to $(n - n_o)^2/c^2$.

The fluorescence and absorption corrections given in Eq. (5) were applied to all of the data obtained on fractions of series II and III, and the data for fractions of series I reported previously were recalculated making fluorescence corrections based on the observed value for OD_{xs}^{10} and the proportionality constant K_{F1}. Values of M_w and $\langle s^2 \rangle_{LS}$ obtained are given in Table III. These have all been calculated with $dn/dc = 0.78_5$. A series of measurements is currently in progress to recheck this value.

d. Correlation of the Dilute Solution Parameters. The values of $[\eta]$ are plotted against M_w in Figure 3. The lack of a satisfactory correlation to fit all of the data is believed to reflect in part the unexpected dependence of $[\eta]$ on the solvent. The data with $[\eta]$ in a given solvent certainly correlate among themselves with M_w much better than does the entire set of data. Use of the sparse data on cross-comparisons of $[\eta]$ for a single sample in different solvents suggests the relations:

TABLE III

Light Scattering Parameters for BBB in Methane Sulfonic Acid

Sample	Solvent	$10^{-5}M_w$	$10^{12}\langle s^2\rangle_{LS}(cm^2)$
Whole 51165	001	0.65	7.5
I-3	001	1.59	40.4
I-5	001	0.87	10.0
I-11	001	0.67	13.0
I-18	001	0.42	----
II-1	002	1.26	28.0
II-2	002	0.70	17.0
II-5	002	0.38	6.0
II-9	002	0.30	----
III-1	003	1.35	37.2
III-1	003	1.26	29.7
III-2	003	0.85	30.9
III-3	003	0.70	25.5
III-6	003	0.30	----
4-22*	---	0.11	----
2-2*	---	0.11	----

*Unfractionated polymers, both with $[\eta]$ = 0.51 dℓ/g in 96% H_2SO_4 solution, and $[\eta]$ = 0.74 dℓ/g in 004 MSA.

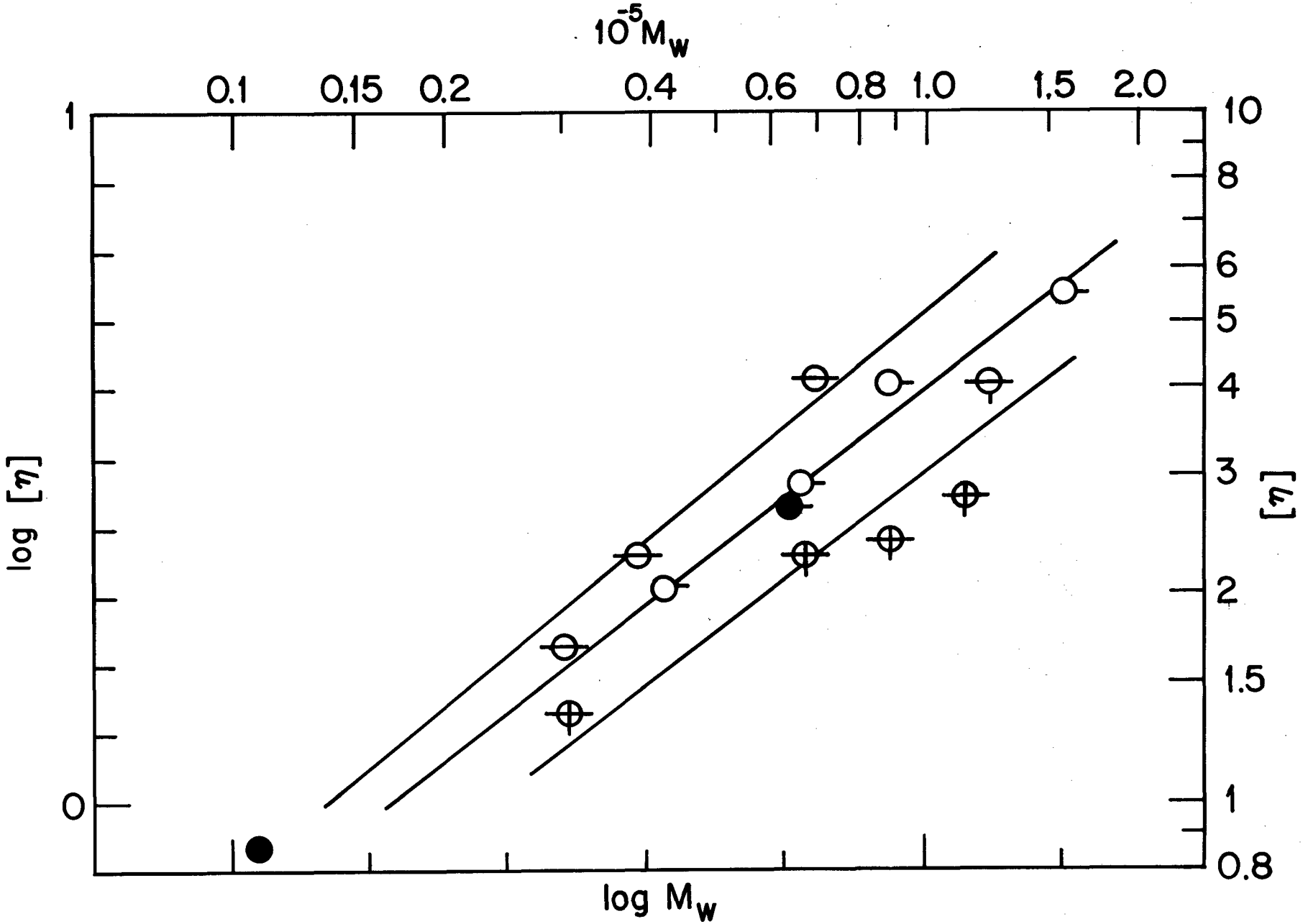

Figure 3. Intrinsic viscosity as a function of molecular weight for BBB fractions in methane sulfonic acid. Symbols: ○ , ⊖ , ⊕ , ● for fractions of series I, II, III, and for unfractionated polymers, respectively; one, two, or three pips for data in batch 001, 002, or 003, respectively, of methane sulfonic acid

$$[\eta]_{001KR} \simeq 1.2 \times [\eta]_{003}$$

$$[\eta]_{001KR} \simeq 0.84 \times [\eta]_{002}$$

$$[\eta]_{001KR} \simeq 0.84 \times [\eta]_{TECH}$$

These relations serve to bring the entire set of data into better agreement. We intend to take further data on $[\eta]$ in a single solvent with several samples with about the same value of M_w (say, I-11, II-5, and III-3) to assess this interpretation.

A second possibility for some lack of correlation among the data is some undetected variation of dn/dc with the solvent. Values of dn/dc are not easy to measure owing to the rapid adsorption of water by the acid. The cell used to measure Δn is capped, but contamination of the sample does occur over a prolonged period. Fortunately, both solution and solvent suffer this contamination, so values of Δn measured not too long after introduction of the samples into the cell may not be too much affected. Measurements are now made with a continuous nitrogen purge of the cell holder housing to slow this contamination. An estimate for the effects of small amounts of water on $\Delta n/c$ is possible. We can expect $\Delta n/c$ to be given approximately by the Dale-Gladstone approximation to the law of additive molar refractivities. That is, the relation

$$\frac{n^2 - 1}{n^2 + 2} = \sum_i \frac{n_i^2 - 1}{n_i^2 + 2} \varphi_i \qquad (13)$$

reduces to

$$\frac{\Delta n}{c} \equiv \frac{n - n_1}{c} \cong \frac{n_2 - n_1}{\rho_2} \qquad (14)$$

for a two component system for which $n_2 - n_1$ is small. Here n is the refractive index of the mixture with components with refractive index n_i present at volume fraction φ_i; n_2, and ρ_2 are the refractive index and density of the polymer; n_1 is the refractive index of the solvent; and c is the polymer concentration in g/cc. Thus, the change of $\partial n/c$ with n_1 is simply:

$$\frac{1}{(\Delta n/c)} \frac{\partial(\Delta n/c)}{\partial n_1} = -\frac{1}{(n_2 - n_1)} \qquad (15)$$

Consequently, a change in n_1 of $\pm \Delta n_1$ refractive index units will cause a change in $\Delta n/c$ of:

$$\pm 100 \frac{\Delta n_1}{n_2 - n_1} \text{ percent.}$$

Setting $n_2 - n_1 \sim 1$, which is about the value for BBB in MSA, and $\Delta n_1 \sim 0.02$, which corresponds to a very large change in n_1, the change in $\Delta n/c$ is seen to amount to only 2 percent. This would correspond to only a four percent change in M_w. Consequently, owing mostly to the relatively large value of $\Delta n/c$ for BBB in MSA, we do not regard solvent effects on $\Delta n/c$ as a probable source of large error in M_w values.

The solvent effects must be more thoroughly investigated and means to suppress them found. Some anticipated steps in this direction have been mentioned above. In addition, we will prepare a sample of MSA with no 282 nm absorption band and a sample of dry methane sulfonic acid anhydride. These will be used in an attempt to determine the extinction coefficient of the anhydride in MSA and the refractive index increment of the anhydride in MSA. With this information, it may be possible to obtain the rate of formation of the anhydride in MSA and to assess its affect on $\Delta n/c$ for BBB in MSA and on $[\eta]$.

The third, and potentially most interesting, possibility for a real lack of a single correlation of $[\eta]$ with M_w for all of the data from Series I, II, and III resides in the method of fractionation. Series I and II were fractionated according to molecular size by exclusion chromatography, whereas fraction III was fractionated from solution according to solubility characteristics of the species present. We can not yet say whether these two methods of fractionation produce entirely equivalent results.

Values of $\langle s^2 \rangle_{LS}$ are plotted against M_w in Figure 4. The light solid line drawn on the graph for reference purposes represents the relation

$$10^{18} \frac{\langle s^2 \rangle_{LS}}{M_w} = 245 \text{ (cm}^2\text{)} .$$

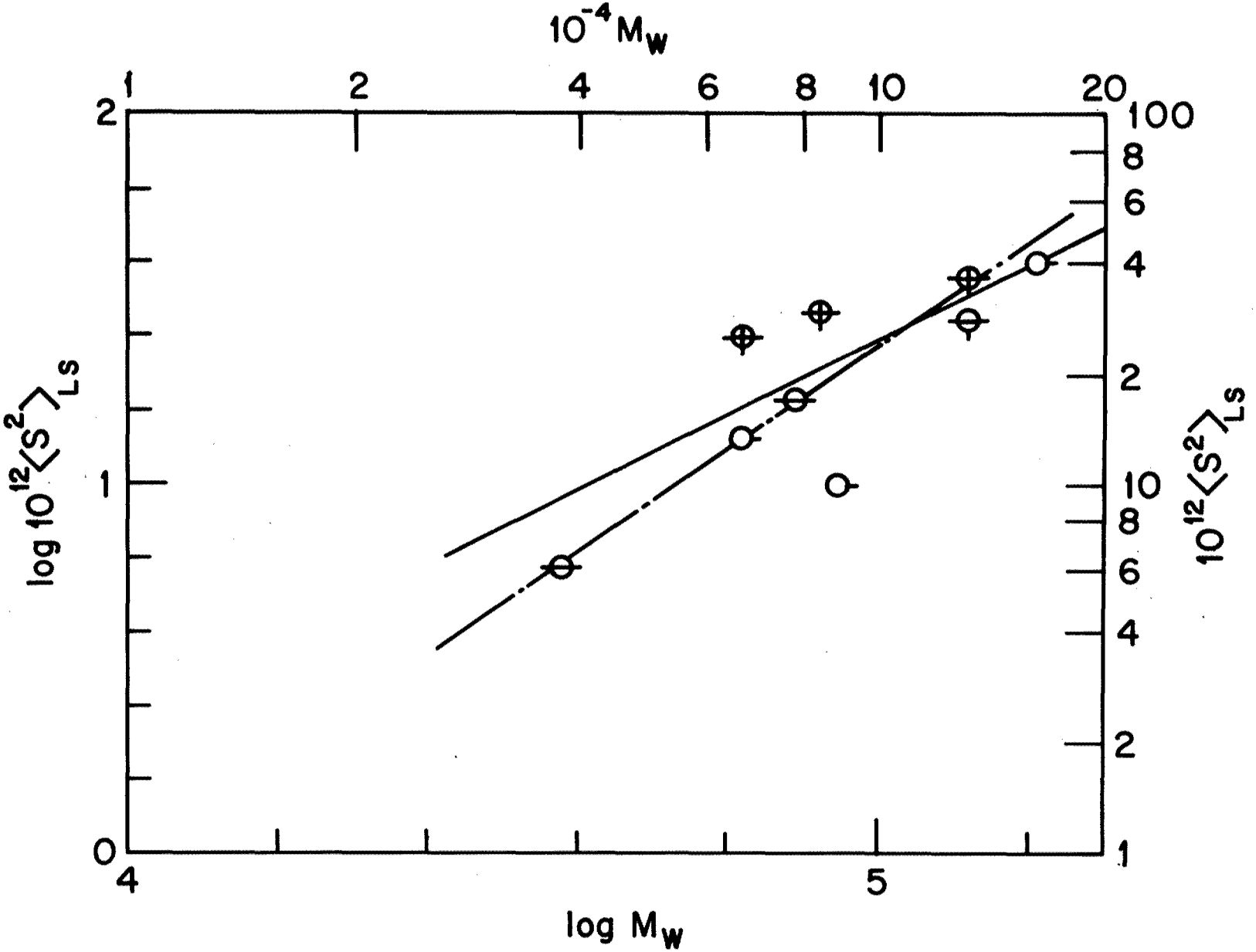

Figure 4. Mean square radius of gyration as a function of molecular weight. The symbols are described in the caption for the previous figure

The data for fractions III may be too high because of the effects of molecular weight heterogeneity on $\langle s^2 \rangle_{LS}$. Although $\langle s^2 \rangle_{LS}$ may depend on $M_w^{1+\epsilon}$ with ϵ slightly greater than zero; the present data do not allow a definitive assignment of ϵ except to indicate that it is not greater than 0.4--the chain line in Figure 4 illustrates $\langle s^2 \rangle_{LS} \propto M_w^{1.4}$. Thus, the dependence of $\langle s^2 \rangle_{LS}$ on M_w is typical of that anticipated for a flexible coil in a good solvent. If we set

$$\frac{\langle s^2 \rangle}{N} = \frac{1}{6} N \ell^2 q^2 \tag{16}$$

where q^2 is comprised of <u>both</u> the short and long range effects on $\langle s^2 \rangle$, and N is the <u>actual</u> number of repeat units of length ℓ, then the estimate 245 for $10^{18}\langle s^2 \rangle_{LS}/M_w$ yields

$$\ell q = 77.5 \text{ Å} ,$$

or

$$q = 4.5$$

if ℓ is taken to be 17 Å. This is certainly a reasonable magnitude for q. On the other hand, a nondraining coil would be expected to have an intrinsic viscosity equal to[5]

$$[\eta]_{ND} = \Phi \left(\frac{\langle s^2 \rangle}{N} \right)^{3-1/2} \frac{N^{1/2}}{m_s} = 6^{3/2} \Phi (\ell q)^{3/2} \frac{N^{1/2}}{m_s} \tag{17}$$

where m_s is the molar weight of a repeat unit. Insertion of the pertinent values leads to an estimate of 47 $d\ell/g$ for the intrinsic viscosity of a polymer with $M_w = 10^5$, compared to the value of ca. 4 found experimentally. A free draining coil would be expected to have an intrinsic viscosity equal to[5]

$$[\eta]_{FD} = \frac{N_a}{600 \, \eta_0 m_s} \langle s^2 \rangle \zeta \tag{18}$$

where ζ is the friction factor per repeat unit, η_0 is the solvent viscosity and N_a is Avagadro's Number. On the assumption that ζ is

related to a Stoke's diameter D_s by

$$\zeta = 3\pi \eta_0 D_s , \tag{19}$$

this reduces to

$$[\eta]_{FD} = \frac{3\pi N_a}{3600} \cdot (\ell q)^2 D_s N/m_s , \tag{20}$$

which yields the value

$$[\eta]_{FD} = 5.64 (10^8 D_s)$$

for a polymer with $M_w = 10^5$ (with D_s in cm). Thus, $[\eta]_{FD}$ calculated in this way is also much larger than the observed value of $[\eta]$ for any reasonable value of D_s.

Part of the discrepancy between measured and calculated values of $[\eta]$ may reside in polydispersity effects on $\langle s^2 \rangle_{LS}$, which would tend to make the calculated values of ℓq too large, but this effect cannot be expected to be as large as the observed discrepancy. We will defer further discussion of this behavior pending resolution of the correlation between $[\eta]$ and M_w.

2. Solutions in Aqueous KOH

Owing to the large correction for absorption and fluorescence necessary to analyze light scattering data obtained in MSA, it is desirable to measure M_w in a second solvent system, preferably free of these effects. The solutions of BBB in aqueous KOH are free of the absorption (and consequently, the fluorescence) corrections, but introduce a new set of complications. Relatively low molecular weight BBB can be completely dissolved in a 4.3 KOH solution, but high molecular weight samples will not dissolve directly in this solvent, although they will remain soluble if treated first with a stronger base or with ammonium hydroxide. Thus, a dialysis step would be very desirable for studies on the high molecular weight samples to bring the concentration down to 4.3 M KOH or less (the KOH concentration must exceed 3.2 M KOH to maintain solubility of BBB). For high molecular weight samples, even the minimum KOH concentration is high enough to 'salt out' the polymer, so that there is an upper limit to the molecular weight that can be measured in this solvent. In addition, specific binding of ions to BBB can be

expected to complicate the interpretation of the data (cf. reference 6). Thus, the usual relation for the dependence of Rayleigh's ratio R on concentration and M becomes in the case of a three component system

$$\frac{K\left(\frac{\partial n}{\partial c}\right)^2_{P,T,m_3} c_2}{R} = \frac{1}{\Omega^2 M_2}\left[1 + o(c_2) + \ldots\right] \tag{21}$$

neglecting intramolecular interference effects, where K is the usual parameter. Here 1, 2, and 3 are the major solvent species (e.g., water), the solute (e.g., the polymer), and the minor solvent species (e.g., KOH), respectively. The refractive index increment $(\partial n/\partial c)$ is taken at constant salt molality m_3 and the factor Ω is related to 'binding' effects of the solvent on the solute. In the limit as c_2 goes to zero; this reduces to

$$\lim_{c_2 \to 0} \frac{K\left(\frac{\partial n}{\partial c}\right)^2_{P,T,m_3} c_2}{R} = \frac{1}{(\Omega^\circ)^2 M_2} \tag{22}$$

with

$$\Omega^\circ = 1 + \frac{\Psi_3^\circ \xi^\circ}{V_m(\partial n/\partial c_2)_{P,T,m_3}} \tag{23}$$

Here V_m is the volume of 1 kg of solvent, Ψ_3° is the refractive index increment

$$\Psi_3^\circ = \left(\frac{\partial n}{\partial m_3}\right)_{P,T,m_2} = 0$$

and ξ° is the 'binding parameter' giving the moles of 'bound' KOH per mole of repeat units

$$\xi^\circ = m_s\left(\frac{\partial m_3}{\partial m_2}\right)_{P,T,m_3}$$

with m_s the molar weight of a polymeric repeat unit. The factor Ω° reduces to unity if Ψ_3° is zero since effectively the bond ions do not scatter any radiation. In the present instance, Ψ_3° is of the order 8×10^{-3} (Kg/g.mol.).

Light scattering and $(\partial n/\partial c_2)_{T,P,m_3}$ determinations on sample 4-22 (cf. Table III) gave the results $(\partial n/\partial c_2)_{T,P,m_3}$ equal to 0.35 (cc/g) with m_3 = 4.3 M KOH, and

$$(\Omega^\circ)^2 (M_2)_w = 1.92 \times 10^4$$

By comparison, the value of M_w quoted in Table III is 1.1×10^4, or Ω° must be equal to about 1.3 according to these data. Insertion of the estimate $\Psi_3^\circ = 8.3 \times 10^{-3}$ yields an estimate for ξ° of 0.0135, or a 'binding parameter' of

$$\left(\frac{\partial m_3}{\partial m_2}\right)_{P,T,\mu_3} = 5.5 \text{ g.mol KOH/g.mol repeat unit.}$$

Although this is a reasonable value for $\partial m_3/\partial m_2$, it will be very desirable to either estimate $\partial m_3/\partial m_2$ by an independent method, or to eliminate the binding effect.

It has been shown[6] that a much simpler result obtains if the refractive index increment $(\partial n/\partial c_2)_{T,P,\mu_3}$ is used instead of $(\partial n/\partial c_2)_{T,P,m_3}$. In this case, the light scattering result reads

$$\frac{K(\partial n/\partial c_2)^2_{T,P,\mu_3} c_2}{R} = \frac{1}{M_2}\left[1 + 2A_2 c_2 + \ldots\right] \qquad (24)$$

which is just the relation normally encountered. The refractive index increment $(\partial n/\partial c_2)_{T,P,\mu_3}$ can be measured directly if the solutions are dialyzed against a salt containing dialyzate and Δn measured for the dialyzed polymer solution relative to the dialyzate. Unfortunately, the usual dialysis membranes are not suitable for 4M KOH solution. It may be possible to use a sintered teflon membrane, however, and experiments along these lines are now in progress.

If dialysis proves to be impossible, then an independent measure of $(\partial m_3/\partial m_2)_{P,T,\mu_3}$. This should be possible by isopiestic measurements of the activities of H_2O in the solution. Possible experimental methods to achieve this end, if dialysis cannot be carried out, are being investigated.

II. Cryoscopy on Sulphuric Acid Solutions —— G. C. Berry

An apparatus has been constructed to determine freezing points of solutions in concentrated sulphuric acid. The apparatus includes many of the features of an instrument described by Glascow, Kroskop and Rossini,[7] but is simpler in some respects. A schematic drawing of the instrument is given in Figure 5. The instrument has been used to determine the freezing point depression θ of 100 percent sulphuric acid caused by the solute

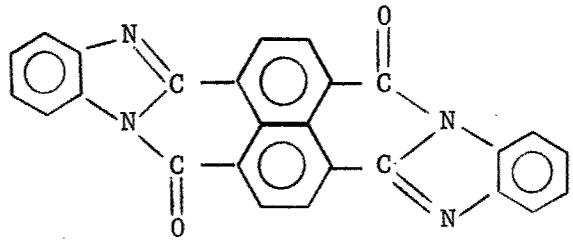

Vat Orange 7

CI. 71105

It will be seen that the value of θ is related directly to the degree of protonation x of the solute S through the reaction

$$S + xH_2SO_4 \rightleftharpoons SH_x^+ + xHSO_4^-$$

The results obtained on Vat Orange 7 yield the value x = 2, suggesting that each of the -N= sites is singly protonated.

1. Description of the Apparatus

Table IV gives some dimensions in the liquid chamber of the instrument. These were selected as a compromise to achieve adequate agitation and still prevent any direct rubbing of moving glass parts. The glass helical stirrer is moved up and down by an external motor and cam arrangement. The glass rods attached to the helix enter the cryostat through rubber seals made from rubber balloons. The liquid chamber holds about 50 cc. A minor difficulty was encountered in the operation of the instrument when small crystals would occasionally get lodged on the shoulder in the liquid chamber which was actually above the solution level. This effect was most

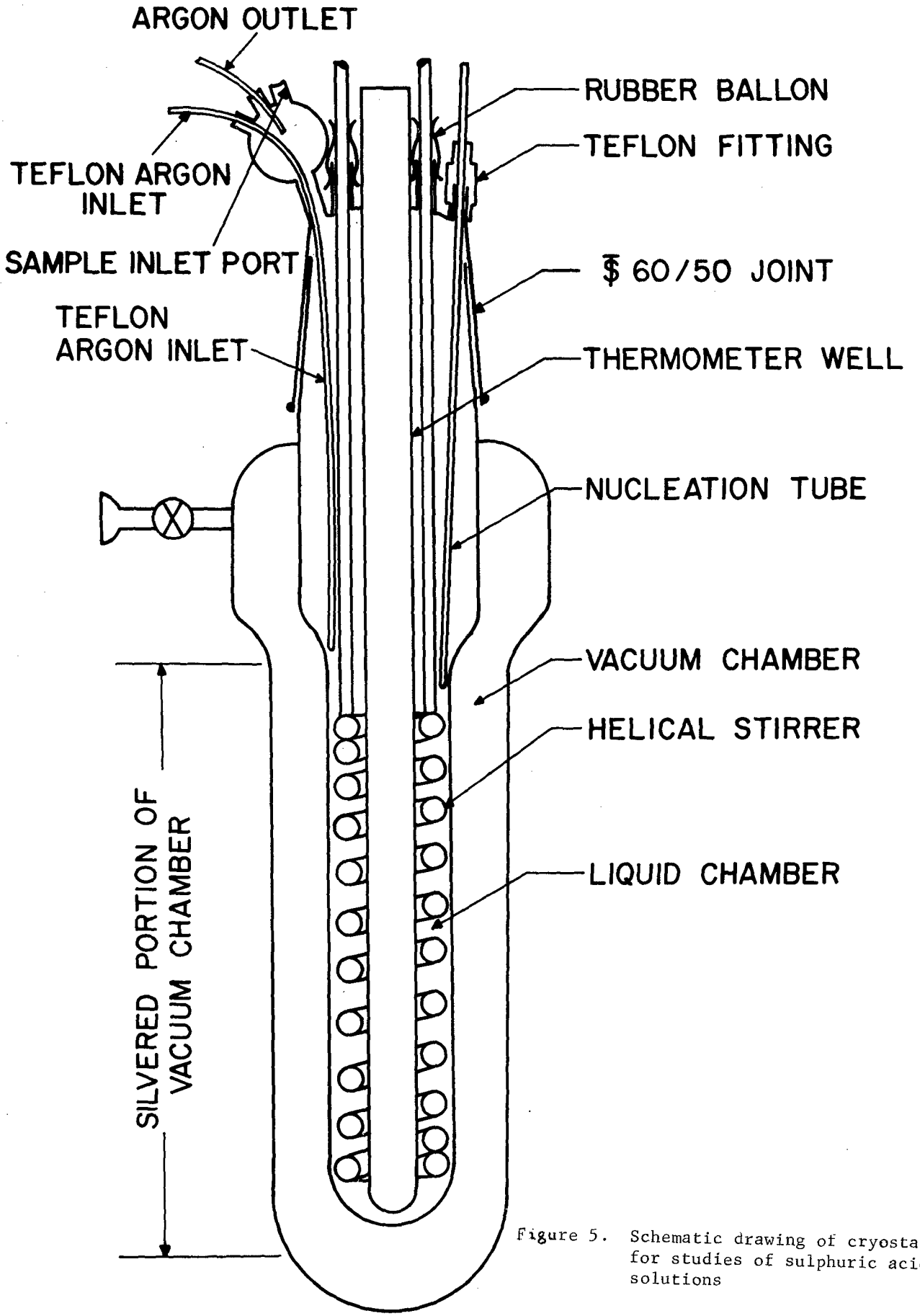

Figure 5. Schematic drawing of cryostat for studies of sulphuric acid solutions

TABLE IV

Some Instrument Dimensions in the Liquid Chamber

Part	Diameter
Thermometer well	13 mm OD
Helical stirrer	15 mm ID; 23 mm OD
Liquid chamber	28 mm ID

pronounced if the stirring action was too vigorous, but was an everpresent problem. These crystals would eventually slide into the liquid, causing a preceptible temperature change. This shoulder can, and should be, eliminated in any revised instrument, but causes no great difficulty as it is. Crystal growth is initiated by placing some frozen CO_2 in the nucleation tube and lowering it through the teflon fitting until it touches the liquid (the nucleation tube need not be removed from the liquid chamber for this operation, so that moisture condensation is no problem).

In use, the liquid chamber was purged exhaustively with dry argon passed into the liquid chamber through a teflon tube and leaked out at the top of the instrument. The sample was then inserted from a syringe through a teflon needle passed through a port at the top of the apparatus. Alternatively, the sample was forced from a graduated cylinder through a teflon tube into the port by the use of dry argon to pressurize the graduated cylinder.

The liquid chamber is enclosed by a vacuum chamber that may be evacuated to adjust the heat transfer rate from the liquid chamber. In practice, the lower portion of the cryostat is immersed in a controlled temperature bath and the pressure in the vacuum chamber is adjusted to achieve the desired rate of heat transfer between the bath and the liquid chamber.

The chamber was tested by repeated determinations of the freezing temperature of a batch of 100 percent sulphuric acid over a period of twenty days. The freezing temperature changed by 0.005°C/day over this period, which amounts to a moisture uptake of 0.001g/day in a 80 g charge. The vessel was kept under a slow dry argon flow during this period. Part of this moisture uptake may reflect dehydration of the walls in the liquid chamber. In any case, this amount of moisture uptake is inconsequential for our purposes.

A platinum resistance thermometer capable of measurement to 0.0001°C was used to measure the temperature. The thermometer was immersed in acetone in the thermometer well. This thermometer provides more than the required precision for our purposes.

2. Experimental Procedure

The freezing point depressions are most easily interpreted if the solvent is 100 percent sulphuric acid rather than an acid slightly richer in water. Thus, a batch of 100 precent sulphuric acid was prepared by combining 96 percent sulphuric acid and fuming sulphuric acid to achieve a freezing point of 10.364, compared to 10.371 for the 100 percent sulphuric acid. This involved sequential addition of the fuming sulphuric acid with a determination of the freezing temperature after each addition. Care must be taken to avoid passing through the desired end point since the freezing point is a maximum for the 100 percent sulphuric acid. The final acid was stored in a sealed flask

and was removed through fittings put together with teflon tubes and Hamilton teflon valves with luer joints. A syringe was used to transfer the liquid from the storage flask to the liquid chamber.

The freezing point of the freshly prepared acid was 10.364°C, with a satisfactory margin of the accepted value 10.371°C. The freezing point of the acid was 10.375 after fifty days of storage, when all tests on the solute reported herein were completed.

Approximately the desired amount of solute was dried in an ampoule at 110°C for 24 hours under high vacuum. The ampoule was then weighed and the solute transferred to a dry graduated cylinder equipped with a special top to allow the introduction of the solvent through a teflon tube. The ampoule was re-weighed to give the weight of solute to ± 0.0002 g. The graduated cylinder was weighed, filled with the required amount of solvent and reweighed to determine the weight of the solution to within 0.001 g. This solution was then transferred to the liquid chamber. Care was taken at all steps to prevent contamination by moisture.

The freezing temperature of the solvent and the solutions were all determined by melting experiments. The instrument was placed in a -78°C bath (isopropanol and dry ice) and the pressure in the vacuum chamber adjusted to achieve a cooling rate of 2.5 to 3 min/°C. Cooling was continued after nucleation until about 10 to 15 percent of the sample was frozen in the form of small crystals. Agitation was still good at this point. A 50°C bath was then substituted for the -78°C bath and the pressure in the vacuum chamber was adjusted to achieve a 2.5 min/°C heating rate. The temperature was measured at one minute intervals. Figure 6 shows a schematic diagram of the temperature profile with the curvature for $T < T_m$ and in the region around T_m greatly exaggerated for clarity. The temperature increases at about the rate 0.4°C/min after the time t_C when all crystals have been melted. The upward curvature between t_B and t_C reflects departure from thermodynamic equilibrium in the system and precludes direct observation of the melting temperature T_m. A smooth curve placed through the data from t_A to t_B should fit the relation:

$$T_{obs} = T_m^{o} - \frac{a}{1 - r} - \frac{b}{(1 - r)^2} \qquad (25)$$

derived from energy balance considerations.[8] Here a and b are constants, of the solute-solvent system, T_{obs} is the observed temperature when a fraction r of the solvent is crystallized, and T_m^{o} is the melting temperature extrapolated to r = 0. After it is assumed that r is proportional to the time measured from the time for which r = 0 so that

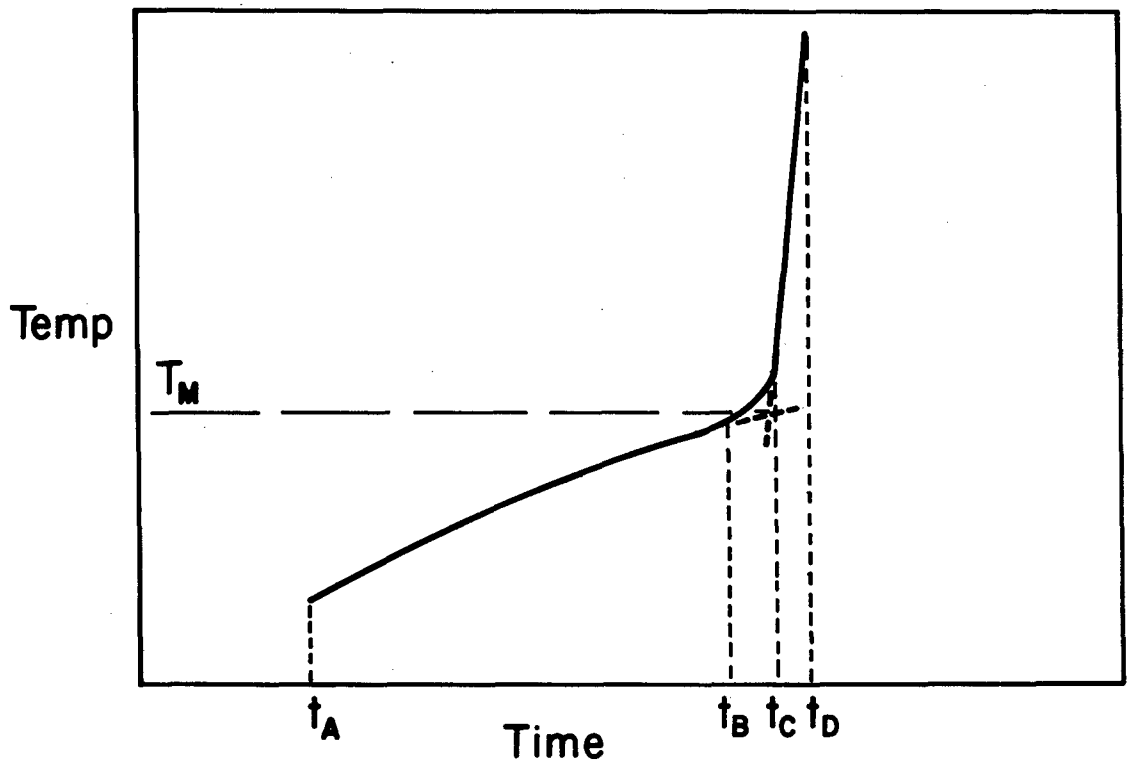

Figure 6. Schematic illustration of a melting curve. The curvature is exaggerated somewhat between t_A and t_B, and greatly between t_B and t_C

$$r = k(t - t_0) , \tag{26}$$

the above reduces to the three parameter (T_m^o, k, and k_2) relation

$$T_{obs} = T_m^o - \frac{k_1}{1 - k_2(t - t_0)} . \tag{27}$$

The time t_o is determined by the intersection of linear extrapolations of the lines $t_A t_B$ and $t_C t_D$; the three parameters T_m^o, k_1 and k_2 are then determined by a curve fitting method described in reference 8 . In the systems studied, the extrapolation from the highest value of T_{obs} to T_m^o was typically 0.02°C.

3. Results and Discussion

Melting temperatures of the 100 percent sulphuric acid and several solutions so far tested are given in Table V. In general, the reaction of a solute S with sulphuric acid may be represented by the equation

$$S + n_1 H_2SO_4 \rightleftharpoons n_2 S' + n_3 HSO_4^- + n_4 H_3SO_4^- + n_5 H_2O + n_6 H_2SO_7$$

For example, o-phenylene diamine apparently is diprotonated[9]

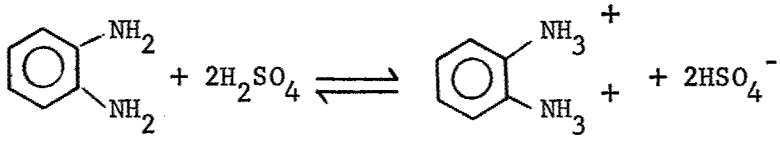

and many carboxylic acids protonate according to

$$RCO_2H + H_2SO_4 \rightleftharpoons RCO_2H_2^+ + HSO_4^- ,$$

although some examples in which a more complicated process occurs are known.[9] Of interest here is the observation that phthalic anhydride is nearly a nonelectrolyte, and that 1,8-naphthalic anhydride is only incompletely protonated. It has been suggested that this behavior may arise from resonance stabilization of the anhydride group, effectively reducing the basicity of the carbonyl group.[9]

TABLE V

Freezing Temperature Data

Solute	Solvent	Solute Molality	T_m (°C)
Vat Orange 7	100% H_2SO_4	0.0037	10.326
Vat Orange 7	100% H_2SO_4	0.0089	10.279
Vat Orange 7	100% H_2SO_4	0.0193	10.088
$KHSO_4$	100% H_2SO_4	0.0121	10.287

Simple ketones are singly protonated similar to carboxylic acids

$$RR'C{=}O + H_2SO_4 \rightleftharpoons RR'C{=}O^+H + HSO_4^-$$

By contrast, methanol and ethanol appear to undergo a more complex reaction, with the first step involving a sulfate formation

$$ROH + 2H_2SO_4 \rightleftharpoons ROSO_3H + H_3O^+ + HSO_4^-$$

with possible protonation of the alkyl hydrogen sulphate.[9]

A measurement on potassium bi-sulphate was made as a check on our procedure. This salt acts as a strong base, being fully ionized

$$KHSO_4^+ \rightleftharpoons K^+ + HSO_4^-$$

It is assumed that Vat Orange 7 reacts as a polybase to give

$$S + xH_2SO_4 \rightleftharpoons SH_x^{+x} + xHSO_4^-$$

The analysis of the freezing point depression θ of solution in 100 percent sulphuric acid is complicated by the self-protonation of H_2SO_4 and by various dissociation species present. Thus, H_2SO_4 dissociates to give the species

$$2H_2SO_4 \rightleftharpoons H_3SO_4^+ + HSO_4^-$$

$$2H_2SO_4 \rightleftharpoons H_3O^+ + H_2SO_7^- ,$$

with further reaction of the ions thus formed also possible:

$$H_3O^+ + HSO_4^- \rightleftharpoons H_2O + H_2SO_4$$

$$H_3SO_4^+ + H_2SO_7^- \rightleftharpoons H_2S_2O_7 + H_2SO_4$$

Fortunately, a great amount of work has been done on this system by now, so that it is possible to treat the data on θ to obtain values of x the degree of protonation (cf., for example, reference). It is convenient to compute θ relative to T_m^o for the hypothetical undissociated acid. The accepted value of T_m for 100 percent sulphuric acid in equilibrium with the various ions listed above is 10.371°C. The freezing point depression $\theta = T_m^o - T_m$ is calculated to be 0.254°C, from knowledge of the concentration of self-dissociation species and the cryoscopic constant k according to the relation

$$\theta + 0.002\ \theta^2 + \ldots = k\phi \sum_i m_i \tag{28}$$

where ϕ is the molal osmotic coefficient, m_i is the molal concentration of species i and the sum extends over all species. Thus, the melting temperature of the hypothetical acid is taken as $T_m^o = 10.625$°C. The cryoscopic constant k is given by

$$k = \frac{R(T_m^o)^2}{10^3 \Delta H_f^o} \ , \tag{29}$$

where ΔH_f^o is the latent heat of fusion per gram, is equal to 6.12 g-mole^{-1}kg for the hypothetical undissociated acid as well as for 100 percent sulphuric acid since contributions from the heat of self-dissociation are negligible.[10] The factor 0.002 arises from a small variation of the heat of fusion with temperature.

The terms in the sum Σm_i arise from the added solute and the ions formed by interaction of H_2SO_4 with the solute, as well as from the self-dissociation of the acid. The latter can be determined from the molal concentrations $m^s_{HSO_4^-}$ and $m^s_{H_3O^+}$ if ions produced by interaction of H_2SO_4 with the solute by use of tables constructed for this purpose based on measurements of the various equilibrium constants involved.[10] Thus, the total molal concentration m_d of self-dissociation species is given to sufficient accuracy by

$$m_d = m_\alpha + m_\beta \tag{30}$$

where m_α is a function only if $m^s_{HSO_4^-}$, and m_β depends only on $m^s_{H_3O^+}$. For Vat Orange 7, $m^s_{H_3O^+}$ is equal to zero and $m^s_{HSO_4^-}$ is equal to xm, where m is the concentration of the solute and x is the degree of protonation. Substitution into Eq. (28) yields

$$\theta + 0.002\ \theta^2 = 6.12\ [m + xm + m_d] \ , \tag{31}$$

or, after rearrangement:

$$1 + x = \frac{\theta(1 + 0.002\ \theta)}{6.12\ m} - \frac{m_d}{m} \qquad (32)$$

for the degree of protonation x. The molal osmotic coefficient has been set equal to unity.[10]

The data in Table V on θ as a function of m for Vat Orange 7 yield the values for x listed in Table VI. The value of x for $KHSO_4$ is 0.98, which is the expected value for this solute. The uncertainty in x arises not from the precision in determination of T_m, but rather from uncertainties in m which are reflected in m_d, and finally the term m_d/m. Figure 7 illustrates the correction terms involved. Solution of Eq. (32) for x is by trial and error since an x value must be assumed to compute $m^S_{HSO_4^-} = xm$ to obtain $m\alpha$, and hence m_d. Fortunately, the calculation converges rapidly to the final answer.

The values of x listed in Table VI are taken to mean that Vat Orange 7 takes up only two protons, probably at the -N= group. This result explains why this solute has such low solubility in H_2SO_4 - H_2O mixtures when the acidity is low enough to remove one proton. It was concluded from our previously reported spectroscopic studies that the pK_B value for the first proton removed in H_2SO_4 - H_2O solvent mixtures was -7, and that rapid aggregation occurred thereafter.

Further studies will include work on Vat Red 15, the cis isomer of the BBB repeat unit, and on low molecular weight BBB fractions. In addition, studies on 3,3'-diaminobenzedene and 1,4,5,8-naphthalene dianhydride would be of interest with regard to the polymerization mechanism of BBB in strong acid solvents. A guess is that the former reactant is fully protonated with x = 4, whereas the latter is only incompletely protonated. Reaction may occur between protonated amine species and unprotonated anhydride groups.

TABLE VI

Degree of Protonation of Vat Orange 7 in 100 Percent Sulphuric Acid

Solute Molality	θ(°C)	x
0.0037	0.299	2.22
0.0089	0.346	1.85
0.0193	0.537	2.24

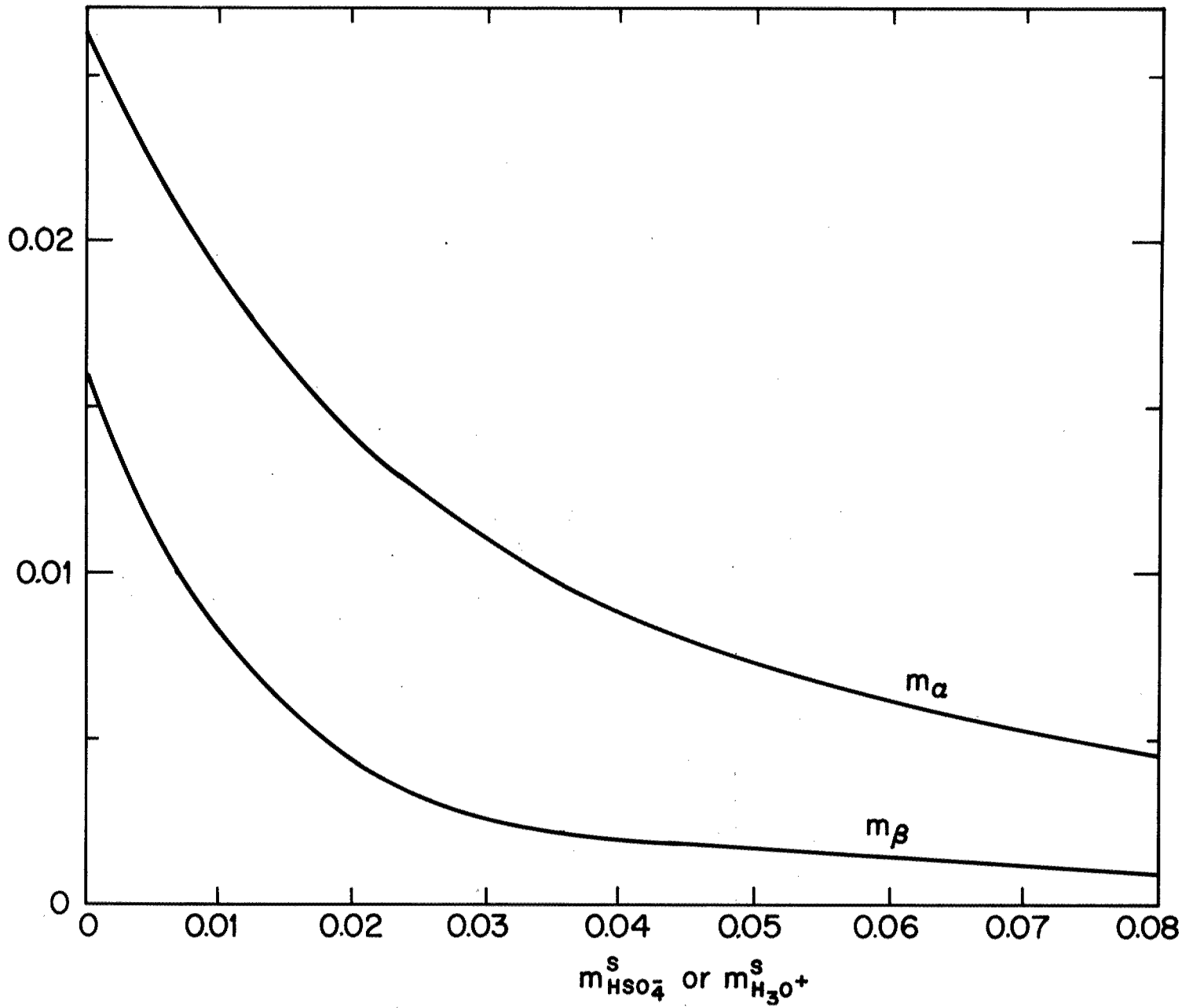

Figure 7. Molal concentrations of self-dissociation species as functions of the molal concentrations of HSO_4^- and H_3O^+ generated by interaction of a solute with H_2SO_4

III. Viscosity of Concentrated Solutions of BBB —— G. C. Berry, J. S. Burke and S. M. Liwak

A. Introduction

The viscosity η of concentrated solutions of BBB-51165 in methane sulfonic acid has been measured as a function of molecular weight M, weight fraction of polymer w_2 and temperature T. Data on nine fractions and two unfractionated polymers have been obtained. Two types of fractions have been used. One set of fractions was obtained with the preparative scale exclusion chromatography column by separation of the eluent into eleven fractions. The second set of fractions was obtained by successive precipitation from an alkaline solution. The data show that for samples at a fixed w_2, $\eta \propto w_2M$ for $w_2M < (w_2M)_c$, and $\eta \propto (w_2M)^{3.4}$ for $w_2M > (w_2M)_c$, where $(w_2M)_c$ is equal to 1150. The dependence of η on w_2 and T appears to be compatible with the usual interpretations; this behavior is discussed below.

B. Experimental

The series II and III fractions used are described elsewhere in this report. Series II fractions were obtained with an exclusion chromatography column and Series III fractions were obtained by successive fractional precipitation from alkaline solution. Samples are designated, for example, as BBB-51165-II; X, or simply as BBB-II; X, where X gives the fraction number. All polymers were dried in vacuum at 100°C before use.

The methane sulfonic acid used was not visibly colored, but was not distilled to remove the impurity band near 282 nm. It is believed that this has no effect on these measurements.

With a few exceptions, viscosities were determined in previously described[11] capillary viscometers slightly modified to prevent moisture contamination. A schematic diagram of the viscometer is given in Figure 8. The device may be sealed for sample storage by connecting ball joints 2 and 3. The capillary height may be adjusted by vertical motion through teflon fitting 1. In use, ball joint 3 is connected to a nitrogen pressure reservoir and ball joint 2 is vented to ambient pressure through a P_2O_5 drying tube. The pressure forces the sample up the capillary and the three rise times between the successive reference marks h_1 to h_4 are measured to ± 0.10 sec. The increments h_ih_{i+1} are spaced to give approximately equal rise times. Calibrated capillaries with a range of bores are available so that the rise time can be held to about 100 sec for viscosities from 1 to 10^6 poise. The applied pressure ΔP is measured on a mercury manostat to ± 0.02 mm Hg. The driving pressure is given by ΔP corrected for the hydrostatic pressure of the sample in the capillary. Values of ΔP used varied from 5 to 30 mm Hg.

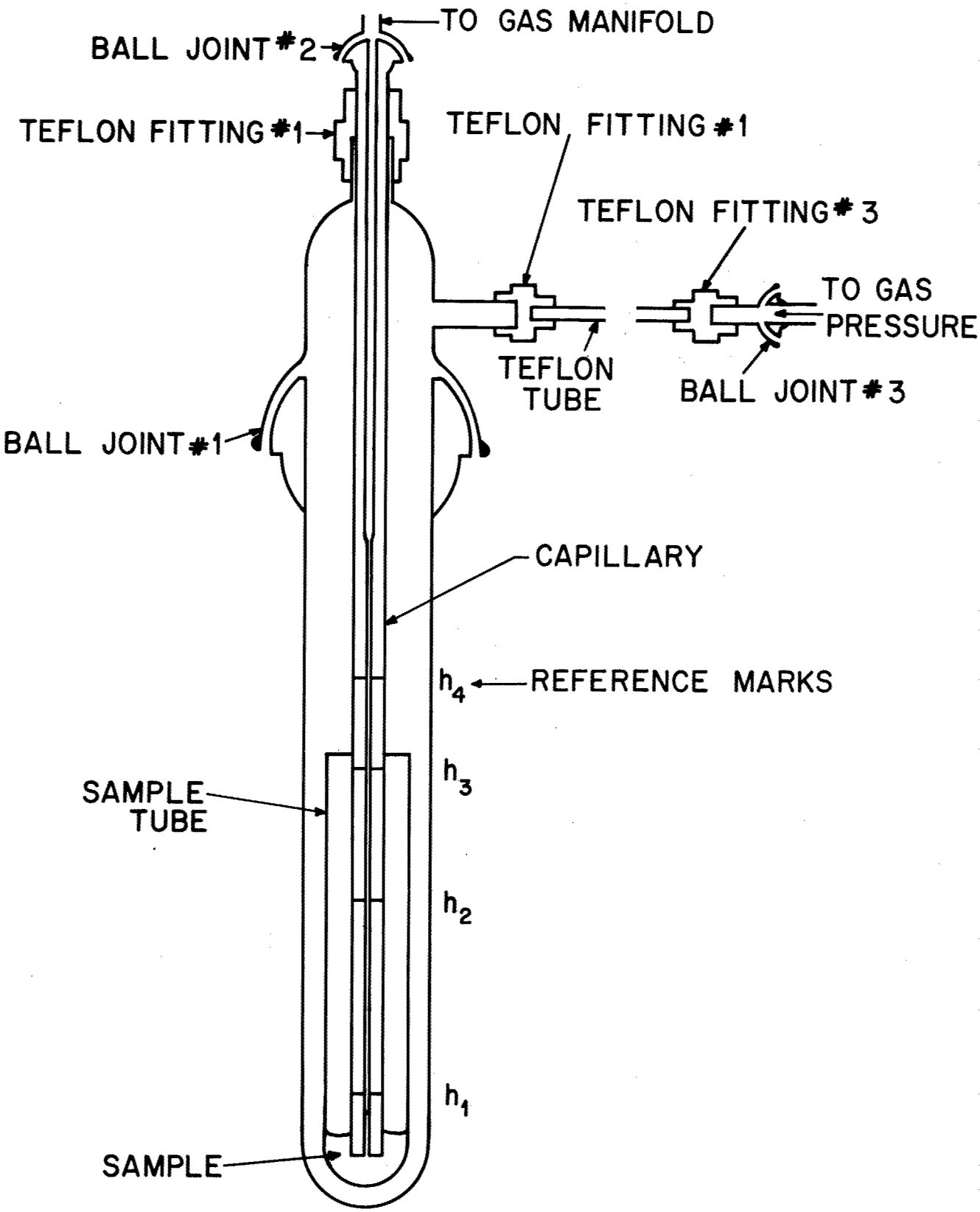

Figure 8. Schematic drawing of the capillary viscometer used to study solutions of BBB in methane sulfonic acid

Samples were prepared by placing the polymer, solvent and a teflon coated magnetic stirring bar in the sample tube. The sample tube was then mounted in a sealed tube such that it turned with the outer vessel as the latter rotated 1 rpm. This assembly was placed in the gap of a magnet in an oven at 40 to 60°C. Rotation of the assembly effected agitation of the dissolving polymer. No stirring was begun until 48 hours after the polymer and solvent were mixed. Complete dissolution usually took several days.

Long term tests revealed no change in the solution viscosity over a period of several days.

C. Results and Discussion

Values of η at 35.5°C are given in Table VII. Figures 2 and 3 show the temperature dependence for two unfractionated samples as a function of w_2, and for one fraction at one value of w_2. The data in Table VII are plotted in Figure 9 according to the usual relation[12]

$$\eta = (Na/6)\ (X/X_c)^a\ \zeta \tag{33}$$

with

$$a = 0 \text{ if } X < X_c$$

$$a = 2.4 \text{ if } X \geq X_c$$

Here

$$X = \left(\frac{\langle s^2 \rangle_0}{M}\right) \frac{\varphi_2 M}{v_2 m_a},$$

where $\langle s^2 \rangle_0$ is the unperturbed radius of the chain and m_a is the molecular weight of a repeat unit. It is usually found that the friction factor per repeat unit ζ can be fitted by the Vogel expression[12]

$$\ell n\zeta = \ell n\zeta_0 - \frac{1}{\alpha(T - T_0)} \tag{34}$$

where both α and T_0 may depend on w_2, but ζ_0 is usually a constant.

TABLE VII

Viscometric Data on Solution of BBB in Methane Sulfonic Acid at 35.5°C

Sample	w_2	log M*	log η
II-2	0.0260	5.08	1.82
II-3	0.0260	4.96	1.46
II-4	0.0260	4.90	1.17
II-5	0.0260	4.79	1.15
II-6	0.0260	4.72	0.79
II-7	0.0260	4.65	0.74
II-2	0.0100	5.08	0.31
II-3	0.0102	4.96	0.22
II-5	0.0100	4.79	-0.03
II-7	0.0100	4.68	-0.19
III-1	0.0254	4.85	1.14
III-3	0.0253	4.70	0.87
III-6	0.0254	4.49	0.36
III-7	0.0255	4.25	0.02
4-22	0.0356	4.00	0.05
4-22	0.0730	4.00	0.97
4-22	0.139	4.00	2.91
51165	0.00913	4.79	-0.20
51165	0.0164	4.79	+0.36
51165	0.0248	4.79	0.53
51165	0.0393	4.79	1.29
51165	0.0483	4.79	1.87
51165	0.0644	4.79	2.30
51165	0.0849	4.79	3.47
51165	0.0996	4.79	3.85
51165	0.134	4.79	5.20
51165	0.163	4.79	5.75

*Interpolated from [η] versus M where not directly measured.

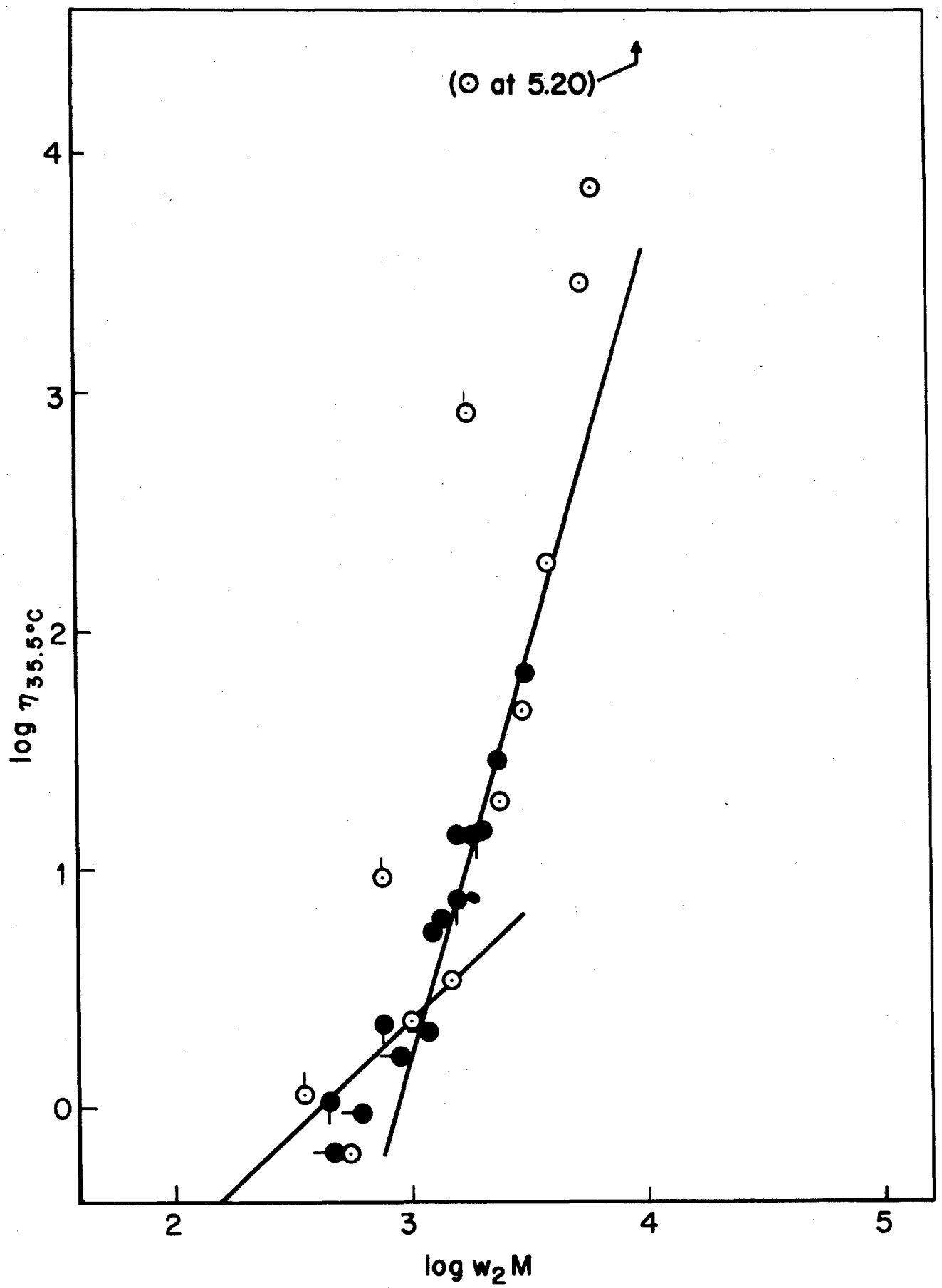

Figure 9. Log $\eta_{35.5°C}$ versus log w_2M for the data in Table VIII. The two lines are fitted to the data for w_2 = 0.026. Data are for BBB-51165, ○ ; 4-22, ○ ; series fractions at w_2 = 0.026, ● ; and 0.010, ● ; and series III fractions at w_2 = 0.025

The friction factor should be a constant independent of M if w_2 and T are held constant at the low values of w_2 of interest. Thus, log η should be linear in log w_2M if samples of different M are examined at one value of w_2. Such data are shown in Figure 9 for $w_2 = 0.026$. The expected change in slope appears to occur for $(w_2M)_c = 1150$. Somewhat unexpectedly, the data for samples with different M, but $w_2 = 0.010$ are significantly below those for $w_2 = 0.026$. This is taken to mean that ζ depends on w_2 but other possibilities must also be considered, cf. seq. A similar conclusion seems to be forced by the data on the unfractionated polymers 4-22 and 51165.

According to Eqs. (33)-(34), the apparent activation energy E_{APP} for viscous flow is given by

$$\frac{E_{APP}}{R} = \frac{d\ell n\eta}{dT^{-1}} = \frac{dX}{dT^{-1}} + a\,\frac{d(X/X_c)}{dT^{-1}} + \frac{d\ell n\zeta_0}{dT^{-1}} + \frac{1}{\alpha\left(1 - \frac{T_0}{T}\right)^2} \qquad (35)$$

Usually, the first three terms on the rhs of Eq. (35) are negligibly small compared to the final term. Under these conditions, E_{APP} depends on w_2 only through the variation of α and T_0 on w_2, and a suspected variation of ζ with w_2 must be accompanied by an apparent activation energy that depends on w_2. In addition, E_{APP} must depend on temperature, unless $T_0/T \gg 1$ over the temperature range studied.

Inspection of Figure 10 shows that E_{APP} does depend on both w_2 and T for sample 4-22. The data shown in Figure 11 also reveal this trend, although these are regarded as being less precise owing to the large values of η and because some were the first data taken with the new instrument before all of the experimental difficulties were completely surmounted.

Analysis of the data in Figures 10 and 11, according to Eq. (34), yields the values for α and T_0 shown in Figure 12. There is considerable latitude in some of the pairs of α and T_0 values at a given w_2 owing to the narrow temperature range of the data in some cases, and to the proximity of T_0 to zero in others. The uncertainty in α after a T_0 is selected is not large, but the pair computed is not necessarily the only choice possible within the experimental error in η, especially as T_0 tends to zero. We somewhat arbitrarily required that the α values, which usually do not vary greatly with w_2, fit a linear relation in w_2, thereby fixing the value of T_0. In no case did this cause disagreement with Eq. (34) outside the experimental error in η. The rapid increase of T_0 with increasing w_2 is noteworthy.

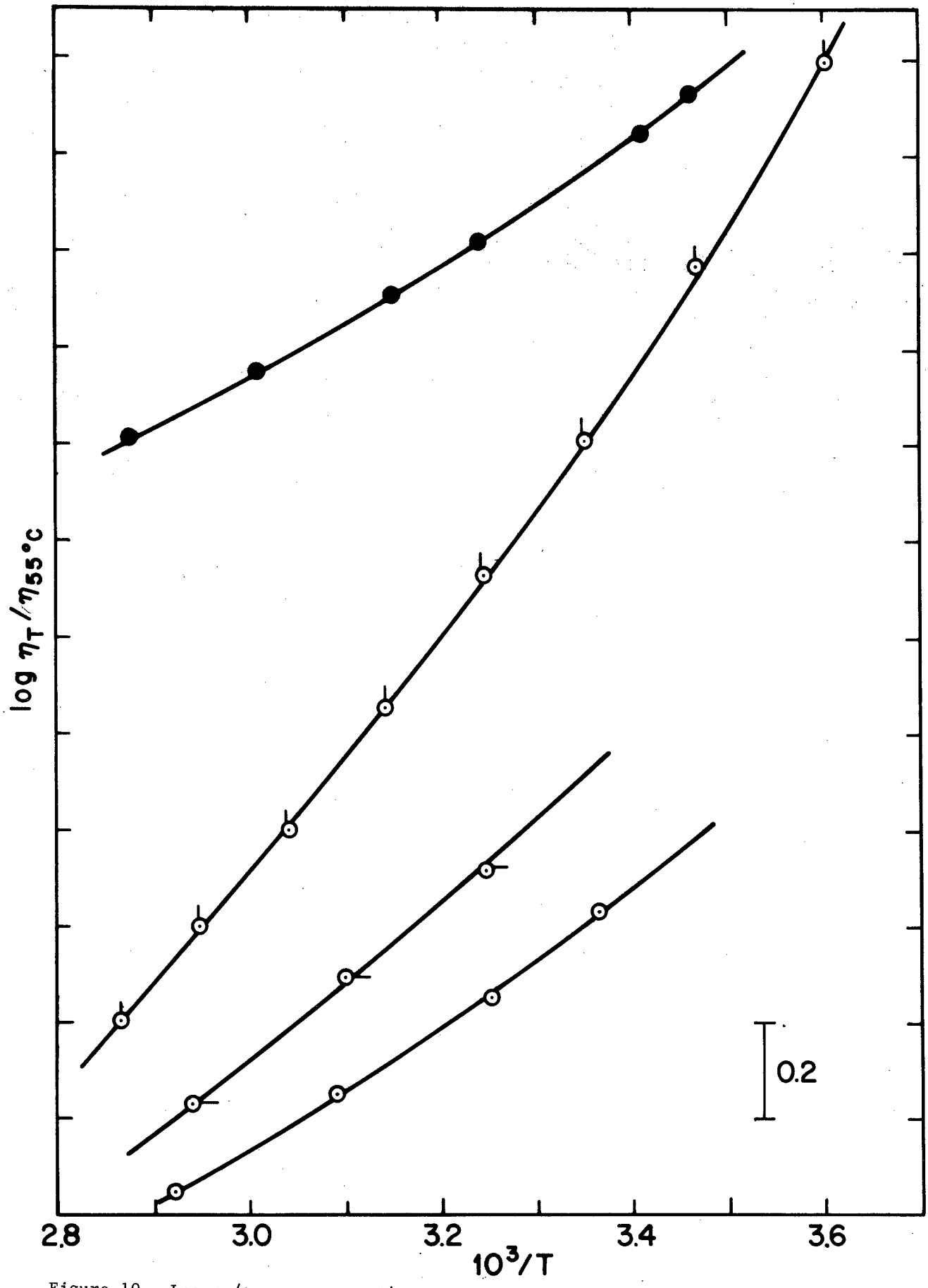

Figure 10. Log $\eta_T/\eta_{55°C}$ versus 1/T for solutions of BBB in methane sulfonic acid: ●, II-7 with w_2 = 0.010; ○, ○–, ○, 4-22 with w_2 = 0.139, 0.0736 and 0.0356, respectively

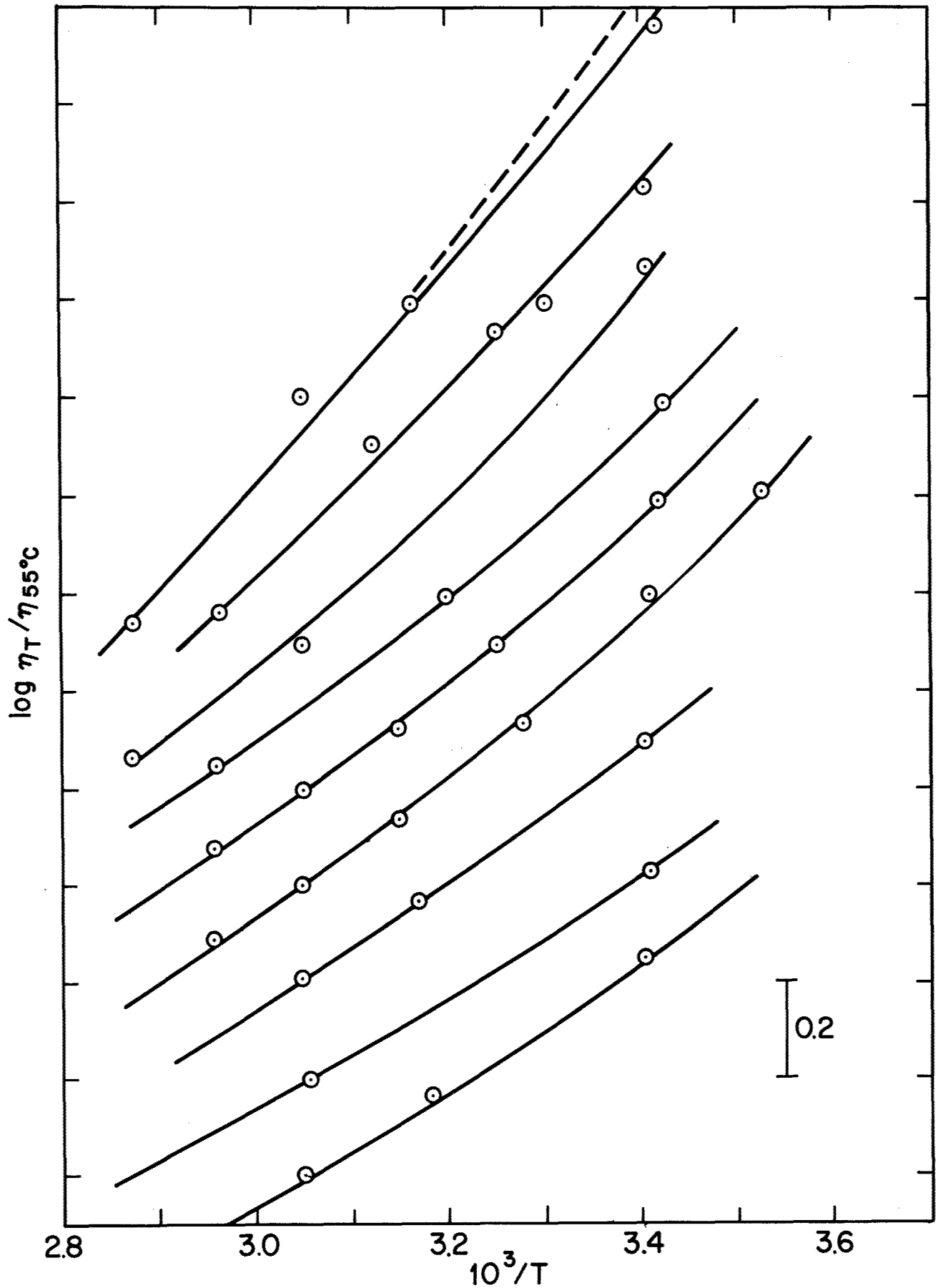

Figure 11. Log $\eta_T/\eta_{55°C}$ versus 1/T for solutions of BBB-51165 in methane sulfonic acid: concentration w_2 from top to bottom are 0.134, 0.0996, 0.0849, 0.0644, 0.0483, 0.0393, 0.0248, 0.0164, 0.00913. The dashed curve on the upper set of data indicates the correlation expected the deviation is within the error of these data

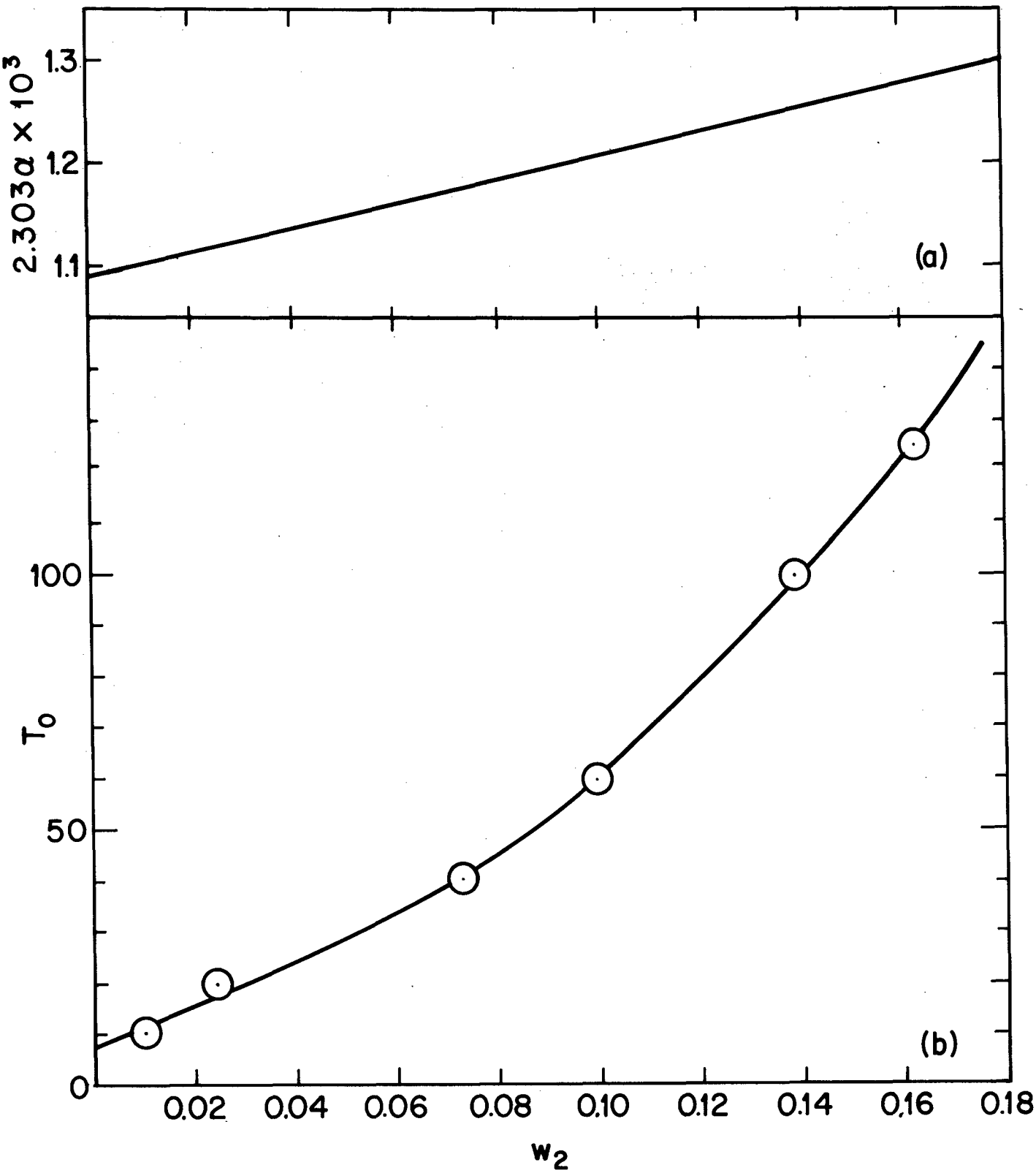

Figure 12. The Vogel parameters α and T_0 for solutions of BBB in methane sulfonic acid as functions of w_2

Figure 13 shows the variation of ζ with w_2 for T = 35°C using the values of η and T_o given in Figure 12. This variation has been used to reduce all of the data in Figure 9 to a common value of log ζ = 3.89, the value for w_2 = 0.025 and T = 35°C. That is, the quantity

$$\log \eta - \frac{1}{2.303\alpha(T - T_0)} + 3.89$$

has been computed for each data point (of course, this is just log η itself for the data on the solutions with w_2 = 0.025 and T = 35°C). This reduced viscosity is plotted against w_2M in Figure 14.

The data in Figure 14 all agree with a single function within experimental error, lending confidence to the assumption that ζ_o and $(\langle s^2\rangle_o/M)$ are indeed independent of w_2, and that Eqs. (33) and (34) can be used to correlate these data on concentrated solutions of BBB. Note that the values of α and T_o necessary for the reduction of the data on the η vs. w_2M correlation came from independent studies of η versus w_2 and T.

The break in slope from a = 0 to a = 2.4 occurs at $(w_2M)_c$ = 1150, a remarkably low value. If we take $\langle s^2\rangle/M$ equal to 20×10^{-17}, m_a = 410, then

$$X_c \sim \frac{20 \times 1150}{410} \times 10^{-17} = 56 \times 10^{-17} ,$$

compared to the value 400×10^{-17} usually observed for more typical systems.[12]

This analysis of the data on concentrated solutions would extrapolate to the extraordinary result that M_c = 1150 for the bulk polymer or that a chain with only three repeat units is already strongly entangled. This conclusion is difficult to understand, and undoubtedly means that these data on moderately concentrated solutions in which the polymer is a charged species cannot be safely extrapolated to give the behavior of the bulk polymer.

According to the theory of F. Bueche,[12] X_c can be represented by the relation

$$X_c = 2\varphi_2^{-1/5} \left[\left(\langle s^2\rangle_0/M \right) \frac{(\varphi_2 M)_e}{v_2 m_a} \right] [Kf(s)]^{-2/5} \qquad (36)$$

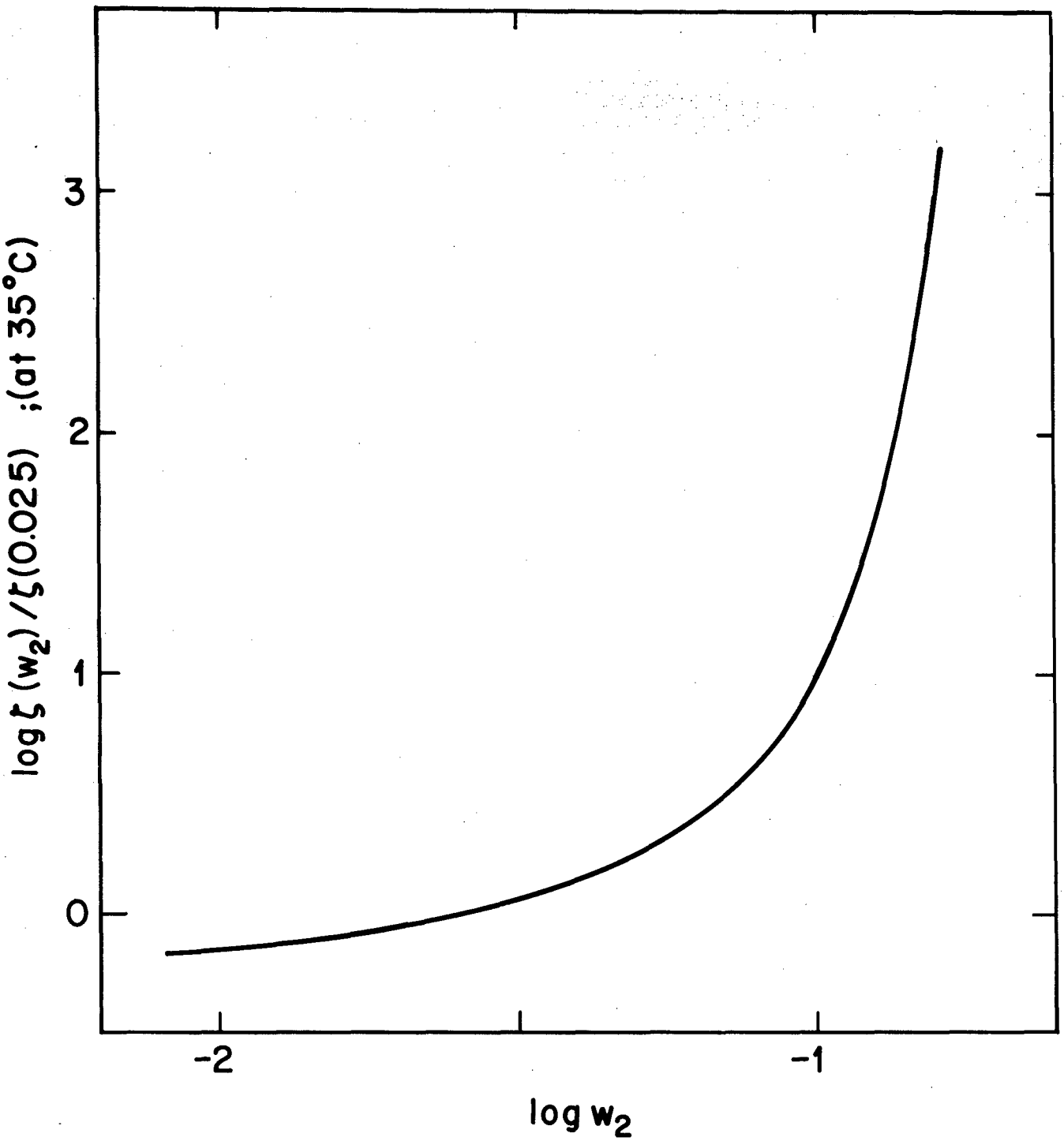

Figure 13. The friction factor as a function of concentration w_2 for solutions of BBB in methane sulfonic acid

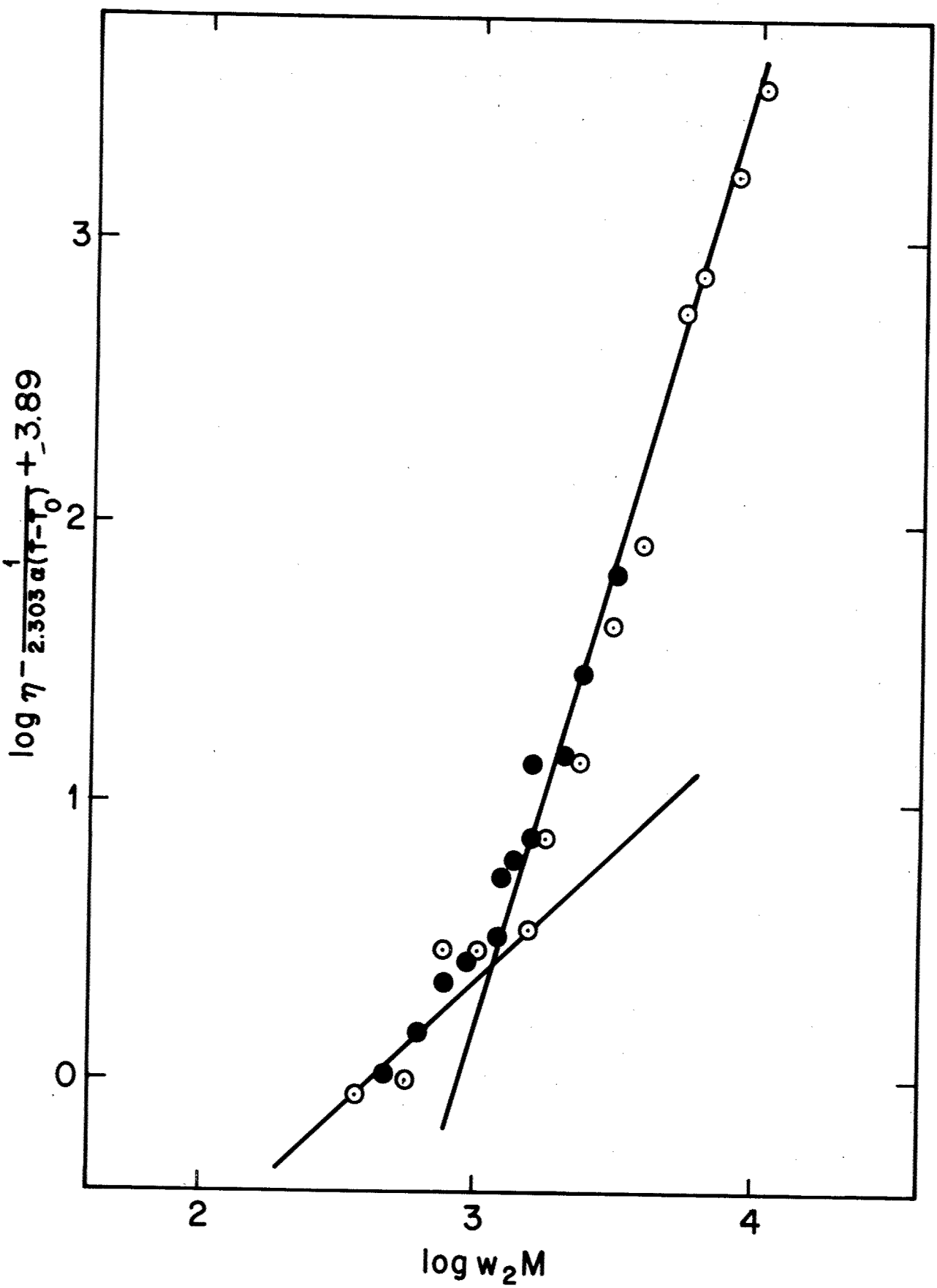

Figure 14. Log η corrected to a common value of the friction factor versus log w_2M. The symbols are defined in the caption to Figure 9.

where $(\varphi_2 M)_e$ is the molecular weight between chain entanglements at concentration φ_2,

$$K^2 = 3(N_0/v_2)^2(\langle s^2\rangle_0/M)^3 M_e \ , \tag{37}$$

and f(s) is the number

$$f(s) = -s + \sum_{n=1}^{\infty} s^n(2n - 1)^{3/2} \tag{38}$$

dependent on the parameter os measuring the strength of the entanglement couple. The parameter S varies between the limits of zero for a couple resulting in no constraint on the molecular motion and unity for a permanent couple. The number f(s) varies from f(o) = 0 to f(1) = ∞, with some representative values being

$$f(0.1) = 0.066 \ ,$$

$$f(0.2) = 0.437 \ ,$$

$$f(0.3) = 0.950 \ ,$$

and

$$f(0.5) = 6.112 \ .$$

Thus, an increase in the strength of the entanglement couple would reduce X_c according to this theory, offering one possible explanation for the low value observed.

Recasting Eq. (36) in a different form, the relation between $(\varphi_2 M)_c$ and $(\varphi_2 M)_e$ is predicted to be

$$(\varphi_2 M)_c = \varphi_2^{-1/5}(\varphi_2 M)_e \frac{2}{[Kf(s)]^{2/5}}$$

For many vinyl polymers, Kf(s) is approximately equal to unity, so that $(\varphi_2 M)_c \approx 2(\varphi_2 M)_e$. An earlier study[13] on the viscoelastic properties of a BBB polymer in methane sulfonic acid ($w_2 = 0.12$) gave an estimated value for the network compliance J_N of 3.2×10^{-6}. The network compliance is usually interpreted in terms of $(\varphi_2 M)_e$ according to the relation

$$(\varphi_2 M)_e \simeq J_N RT/v_2 ,$$

leading to the estimate $v_2(\varphi_2 M)_e = 6.4 \times 10$ so that for these estimates $(\varphi_2 M)_e > (\varphi_2 M)_c$, a result heretofore not formed for any polymer system to our knowledge. This unexpected result is not impossible according to the theory leading to Eq. (36) since a strong intermolecular couple can effect a value of f(s) greater than unity, but it would be very unusual if it proves to be correct.

Further evaluation of this unexpected result will require data other than the viscosity alone, although these data should be expanded to include a wider span in φ_2, T, and if possible, M. The dependence of the viscosity on the shear rate should also be studied, and the stress-strain behavior should be examined as a function of time. Stress "overshoot" phenomenon in the latter method may be of particular value in attempts to assess the strength of the intermolecular couple involved in the chain entanglements. In this measurement, the stress σ is monitored as a function of time t while the sample is sheared at a constant shear rate κ. It is usually found that the sample will initially support a stress greater than the steady state value. The stress decay is thought to be related to a decay of the entanglement density from its static value to steady state value dependent on κ. A kinetic analysis of the decay rate should then provide sone information on the strength of the entanglement couple. The cone-and-plate viscometer described elsewhere in this report has been designe d to carry out such studies. In addition, the existence of a yield stress, if any, can be examined. If present, a yield stress could also be related to the strength of the entanglement couple.

The dependence of ζ on w_2 illustrated in Figure 13 is striking. The rapid increase of ζ with increasing w_2 reflects, of course, the marked increase of T_0 with increasing w_2. It is not possible to quantitatively extrapolate these data beyond the values of w_2 actually measured, but it appears that log ζ is increasing very rapidly with log w_2 at the highest values of w_2 measured, and that this increase is far more rapid than the $w_2^{3.4}$ that comes from η/ζ. If we set $\zeta \propto w_2^n$, then n is not a constant over the span in w_2 investigated, and $n \sim 10$ for the largest values of w_2 studied and can be expected to increase to still larger values with increasing w_2. This very strong dependence of ζ on w_2 is undoubtedly related to the difficulty encountered in attempts to obtain very concentrated solutions of BBB. It is notable that this behavior is independent of M.

It is probable that the large size of the repeat unit of BBB is responsible for the rapid increase of ζ with increasing w_2, although charge effects may also have to be considered. Thus, the analysis given above suggests that the segmental mobility (reflected in ζ^{-1}) decreases very rapidly as the polymer concentration increases. It is of interest to compute the constant ζ_0 for comparison with values typical found for other synthetic polymers. Using Eqs. (33) and (34),

$$\log \zeta_0 = \log \eta_c - \log \frac{NA}{6} X_c - \frac{1}{2303\ \alpha\ (T - T_0)} \quad ,$$

where η_c is the value of η at $X = X_c$ and temperature T. With the value of X_c quoted above and the value of η_c from Figure , we get

$$\log \zeta_0 = -11.26 \ ,$$

which is of the same order magnitude as the value usually found.[12]

The possibility of intermolecular aggregation in concentrated solutions of BBB has been posed previously.[1,2,13]. X-ray diffraction studies have revealed that there is considerable supramolecular structure in films prepared by evaporation from methane sulfonic acid solution. Moreover, it has not been found possible to directly prepare a solution with $w_2 > 0.25$ by direct addition of polymer and solvent. These viscometric data suggest that poor segmental mobility may be the root cause of the poor solubility at high polymer concentrations, and that this effect may be augmented by an appreciable intersegmental attractive interaction tending to stabilize a supramolecular structure once formed.

Future studies planned include the extension of the data to cover a wider span in φ_2, and T, and perhaps M, and to utilize attenuated total reflectance spectroscopy and light scattering to search for evidence of supramolecular structure in the concentrated solutions. In addition, a wide range of studies are planned for the cone-and-plate viscometer involving the details of the stress-strain-time behavior as a function of φ_2, T and M.

IV. Design and Construction of a Cone and Plate Viscometer —— G. C. Berry

A. Introduction

The possibility of using rheological studies on concentrated solutions of BBB to learn more about the intra- and intermolecular interaction in that system has been mentioned in another section of this report, and discussed previously.[2] An instrument to carry out these studies should be able to

1. measure the shear stress as a function of the time of shearing at variable rates of shear,

2. measure the strain induced by an applied shear stress, including the possibility of zero strain for a small finite stress, and

3. be able to do both of the above over as wide a temperature range as possible.

In addition, because of the peculiar nature of the BBB-acid system, the instrument must also

4. protect the sample from contamination by moisture,

5. be able to work with small samples owing to the scarcity of fractions of BBB, and

6. have all surfaces in contact with the sample inert to strong acids.

In our opinion, no instrument available on the market provided all of these features. Moreover, none of the instruments described in the literature which we extensively surveyed fulfilled all of our requirements. Consequently, a new instrument described below has been designed for use with concentrated solutions of BBB. We plan to study the viscosity η and its dependence on rate κ as a function of molecular weight M, polymer volume fraction φ_2, and temperature T. The transient shearing stress σ in the buildup leading to the steady state value of σ will be studied as functions of κ, M, φ_2 and T. The yield stress σ_0, if any, can also be studied as a function of M, φ_2, and T with the proposed instrument.

B. Instrument Description

It is not our intention in this report to provide detailed information on the construction of the instrument, but rather to describe the principal features of the apparatus and its modes of operation. The details of construction will undoubtedly be altered to some degree from the working drawings used in the construction as various unforeseen problems arise. A detailed drawing of the final instrument will eventually be available. A schematic drawing of the

instrument is given in Figure 15 ; the layout of the components in the actual instrument is not that given in Figure 15, which is simplified for clarity. Three of the important features of the instrument have been taken from three separate instruments described in the literature:

1. a yoke Y, to which the cone C is rigidly attached, is suspended in the center of a rigidly mounted frame F by two torsion wires T_1 and T_2;[14] the yoke is free to rotate about the axis of T_1 and T_2,

2. a drag cup motor with field coils M and laminated stator L rigidly attached to the frame F exerts a known and variable torque on a thin aluminum cup K attached rigidly to the yoke Y, so that a torque may be transmitted to the cone C without any frictional losses,[15] and

3. a sensitive differential photodyode to be used with a short optical lever to allow resolution of angular motion of the yoke Y, and hence the cone, to within 10^{-5} radians.[18]

The plate may either be driven at a constant angular velocity through the gear train G_1/G_2 by a motor attached to the shaft D, or the plate may be held stationary. The cone may be held stationary while the plate rotates by providing a torque with the drag cup motor just sufficient to counterbalance the viscous drag generated by a rotating plate, or the cone may rotate through a measured angle by application of a torque with the drag cup motor while holding the plate fixed. Thus, the instrument may be used to study the shear stress σ as a function of shear rate and the time of shearing, or may be used to investigate the existence and properties of yield phenomenon.

No provision for temperature control is indicated in the simplified version of the instrument shown schematically in Figure 15 . In fact the cone is isolated from the frame by a ceramic shaft I, as is the plate from the spindle S. Five concentric aluminum rings E_2 are mounted on the upper side of the cone, cf. Figure 16 ; these rings rotate freely with the cone. These rings are interleaved with five concentric rings E_1 attached to a heat exchanger fixed rigidly to the frame of the instrument. Heat exchange from E_1 to E_2 controls the temperature of the cone C. A similar arrangement is used to control the temperature of the plates.

The plate may be moved along the vertical axis of the spindle S by raising or lowering the spindle housing H in its mounting O. The gear train and spindle move with the spindle housing.

Both cone and plate are gold plated over a stainless steel base to provide protection against corrosion by the strong acids to be studied.

Figure 15

Schematic drawing of the cone and plate viscometer in cross-section illustrating its basic components. The symbols designate instrument components as follows:

F	outer frame
Y	yoke mounted on torsion wires to allow rotation as shown
T_1,T_2	torsion wires suspending yoke in the frame
C	cone attached to yoke
P	plate
I	thermal insulation for cone and plate
S	spindle on which plate is mounted
B_1,B_2	precision spindle bearings
H	spindle housing
O	mount for the spindle housing
G_1,G_2	gears to transmit torque to the spindle
D	drive shaft
B_3	drive shaft bearing
M	field coil of drag cup motor
L	laminated stator of drag cup motor
K	thin aluminum cup of drag cup motor

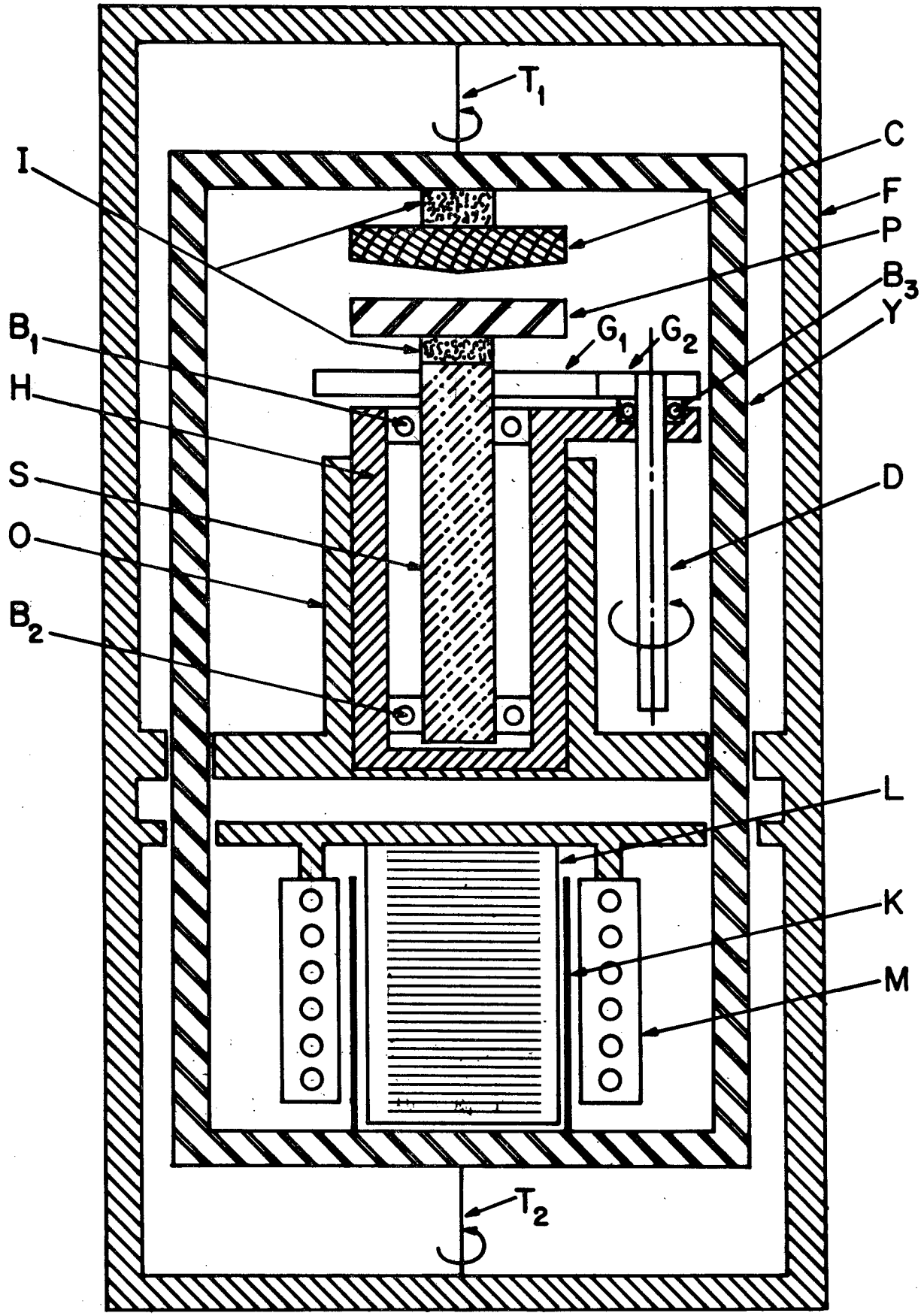

Figure 15. Schematic drawing of the cone and plate viscometer in cross-section illustrating its basic components

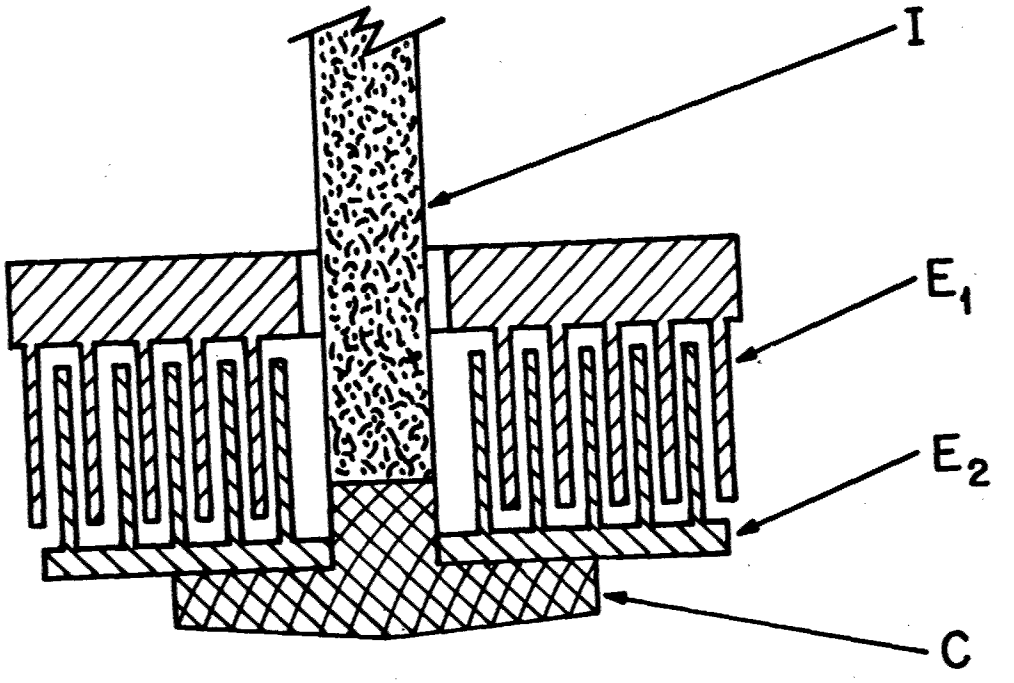

Figure 16. Detail of the heat exchanger for the cone C showing the concentric rings E_2 attached to the cone and the interleaved concentric rings E_1 attached to a fixed heat exchanger

C. Some Design Considerations

Before discussing some of the special precautions necessary in the construction of this instrument, it is useful to consider the effects of several types of misalignments of the cone and plate on the measurable parameters. Calculations of this type have been given by Markovitz, et al.,[17] for the four misalignments shown in Figure 17 . The results are expressed in terms of the total applied torque T, the viscosity η at the shear rate κ, the angular velocity Ω of the rotating member, the angle θ between the perfectly aligned cone and plate and the radius R of the cone and plate.

For the perfectly aligned system,

$$T_0 = \frac{2\pi R^3}{3} \cdot \frac{\eta\Omega}{\theta} = \frac{2\pi R^3}{3} \sigma \tag{39}$$

and,

$$\kappa = \Omega/\theta \tag{40}$$

For a misalignment with the apex of the cone a distance h above the surface of the plate,

$$T = T_0[1 - 3h/2\theta R] , \tag{41}$$

where T_O is given by Eq. (39).

For a misalignment with the axis of the cone tilted by a small angle β with respect to the axis of the plate,

$$T = T_0[1 - (\beta/\theta)^2]^{1/2} ,$$

or

$$T = T_0[1 - \tfrac{1}{2}(\beta/\theta)^2]$$

if $\beta \ll 0$.

For a misalignment with the axis of the cone and plate parallel, but displaced by a distance by

$$T = T_0[1 + 7b^2/3R^2] .$$

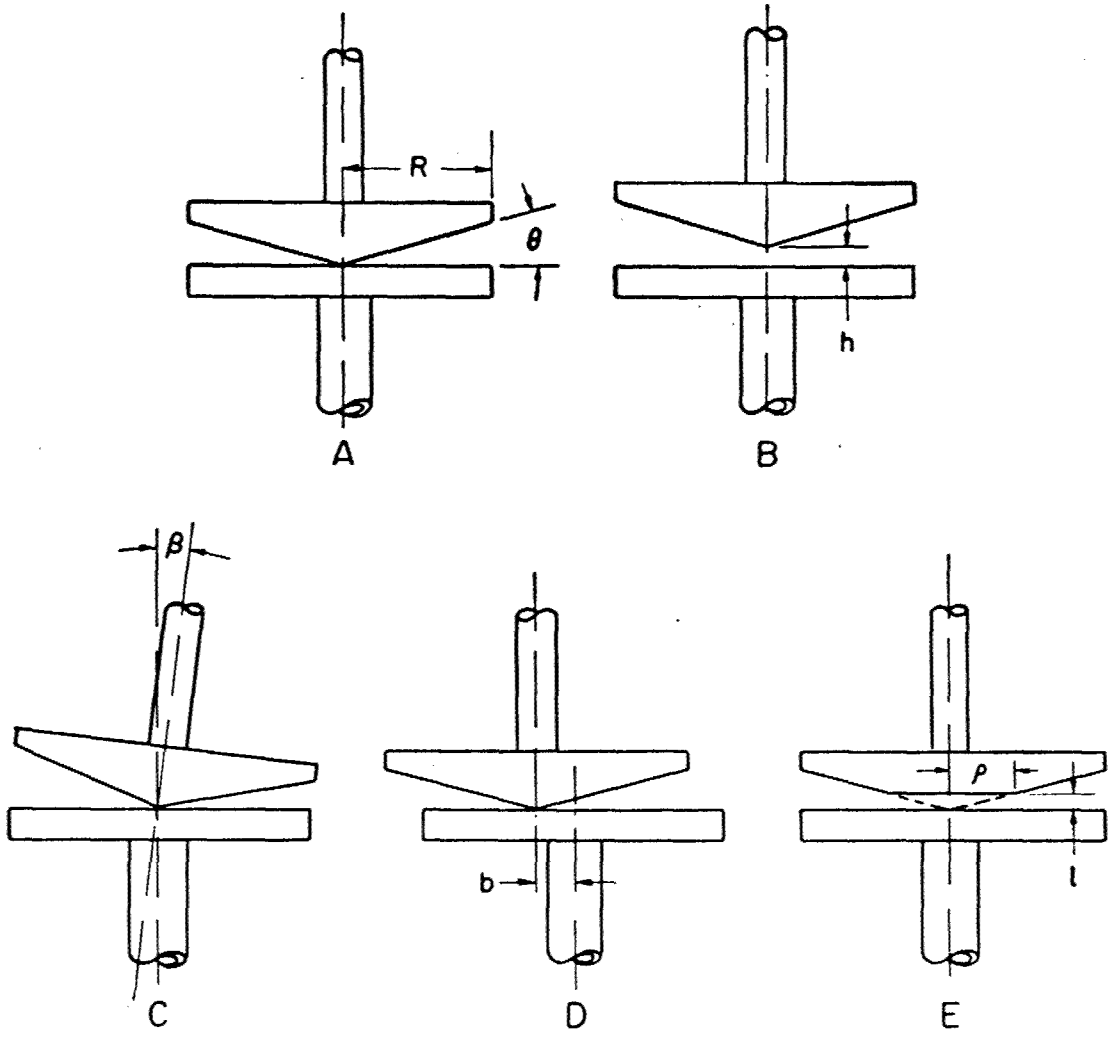

Figure 17. Geometric alignments possible between a cone and plate: (A) correct alignment; (B) vertical displacement; (C) axes not parallel; (D) axes parallel but displaced; (E) truncated cone

Finally, if the cone is truncated so that its plane surface is a circle of radius ρ.

$$T = T_0[1 - \rho^3/4R^3]$$

Thus, the magnitudes of h, β, b and ρ that will each contribute a 1% error to the measured torque are given by

$$h(1\%) = 0.0067\theta R$$

$$\beta(1\%) = 0.14\theta$$

$$b(1\%) = 0.0654R$$

$$\rho(1\%) = 0.34R$$

In the instrument designed here, R = 2 cm and θ = 0.026 rad, thus h(1%) = 0.00035 cm, β = 0.0036 rad = 13 minutes, b = 0.14 cm and ρ = 0.68 cm. The constraint on h is particularly severe, and indicates that special methods will be required to maintain the separation between cone and plate within the required limits.

D. Some Particulars of the Design

The layout of the actual instrument differs from the simplified version shown in Figure 15, and only some of the salient details of the actual design will be discussed. In particular, some of the general methods of construction employed, the fabrication of the spindle, the method used to mount the torsion wires that suspend the yoke, and the design and construction of the drag cup motor will be described.

The frame is constructed from 4 1/4 inch ID-stainless steel pipe with 1/4 inch wall. The yoke is fabricated from 4 inch OD thin wall stainless tubing. The use of round stock permits fabrication on a precision lathe to facilitate the maintenance of close tolerances on critical dimensions. For example, the inside diameter of the spindle housing mount O must be turned after mounting O on the frame to insure that O and the torsion wires T_1 and T_2 are coaxial. The plate must be finished by grinding its surface while rotating the spindle S mounted in its housing H to obtain as true running a surface as possible. Precision ABEC 7 Barden spindle bearings are specified to mount the spindle. Precision Pic helical gears are used to drive the spindle to reduce uneven rotation of the plate as much as possible.

The frame is constructed so that it can be sealed off to allow evacuation of the instrument for effective purging with dry gas. The instrument is not designed to operate under a vacuum, however, since no provision is made to seal the drive shaft when it is rotating.

A critical problem is the selection and mounting of the torsion wires used to suspend the yoke. The optimum material for the wire should have a low value for JG, where J is the polar mount of inertia and G is the shear modulus, since the angular deflection φ to an applied torque T for a wire of length L is given by

$$\varphi = TL/JG$$

On the other hand, the wire should have a high tensile strength so that the yoke can be suspended rigidly with the wires in tension. Since $J = \pi d^4/32$, and the tensile strength is proportional to d^2, a wire with a small diameter, but a large value of Young's modulus E is desirable. Tungston wire has a high E, but is difficult to mount owing to its brittleness. A method has been found to fuse a silver bearing solder bulb onto the nickel plated ends of a tungston wire.[18] These can then be mounted in holders and cemented in place with an epoxy adhesive to give a satisfactory mounting for the wires. Wires 0.010 inch in diameter so mounted have been tested and the mount has been found to be stronger than wire. The wires being used are 0.010 inch in diameter, and have $G = 16.4 \times 10^{11}$ dyne/cm^2 by our measurement, so that

$$\frac{dT}{d\varphi} = 6.7 \times 10^4 L^{-1} \text{ dyne cm/rad}$$

Since L is 10 cm in our instrument, and the resolution anticipated in φ is 10^{-5} rad, we should be able to resolve torques of the order 0.1 dyne cm. With the cone and plate described above, the shear stress that should be resolved is

$$d\sigma = \frac{3}{2\pi R^3} dT = \frac{1}{15.3} dT ,$$

or $\pm$ 0.007 dyne/cm^2. Thus, a shear stress as low as 0.07 dyne/cm^2 could be measured with a precision of $\pm$ 5 percent with the geometry described. Alternate cone and plate assemblies could be used to gain increased sensitivity if necessary.

The maximum shear stress that can be measured is determined by the torque generated in the drag cup motor. A duplicate of the

drag cup motor described in reference 15 was constructed and tested at applied voltages up to 200 VAC to produce a maximum torque of 6×10^4 dyne cm, corresponding to a maximum shear stress of 4×10^3 dyne/cm^2 for the 2 cm radius cone and plate. While this would have been sufficient for a variety of studies, it was felt desirable to extend this limit if possible. Unfortunately, very little in the way of detailed construction principles appears to be available to guide the construction of high torque drag cup motors. Major uses of drag cup motors appear to be as low torque, low inertia, components in rotational transducers. Discussion of the electrical features of these motors can be found in reference 19, but very little was found on other design parameters. A schematic drawing of the electrical components of the motor is illustrated in Figure 18. There are two separate field coils, each with an internal resistance R and an internal inductance L. The torque is related to the currents i_1 and i_2 passing through the separate field coils by the relation

$$T = \frac{1.02 \times 10^7}{\pi N_s} \mu (R_1 R_2)^{1/2} \, i_1 i_2 \sin \theta_{12} \text{ (dyne-cm)} \tag{42}$$

where N_s is the rotational frequency of the revolving field relative to that of the cup in rps, equal to 120/p with p the number of electrical poles for a stationary cup and 60 HzAc voltage, μ is the efficiency factor for the motor, and θ_{12} is the phase angle between the currents in coils 1 and 2. The efficiency factor μ should be independent of the currents i_1 and i_2, and is fixed by the details of the construction of the motor. The prototype motor described above had an efficiency of 10 per cent, which is typical of drag cup motor. The utility of Eq. (42) for our assemblies was tested and found adequate by experiments in which T was measured while i_1, i_2, and θ_{12} were all varied separately.

Efforts to improve μ of the prototype by decreasing the gap between the field coils and the stator did not produce a substantial improvement. Consequently, a larger drag cup motor was constructed utilizing the field coils from a 1/40 HP model NC1-13 Bodine sychronous capacitor run motor. An aluminum cup with a 0.010 with wall thickness and 0.010 inch gaps between coil and cup and between cup and core was employed. This unit produced 5×10^6 dyne cm maximum torque, with an efficiency of 17.5 per cent. This torque corresponds to a shear stress of 3×10^5 dyne/cm^2 for the 2 cm radius cone and plate. This is adequate owing to the characteristics of the dependence η on the shear rate κ. For example, for purposes of estimating the torque requirements for studies on polymeric liquids, we can set

$$\eta = \eta_0 (\kappa_c / \kappa)^a$$

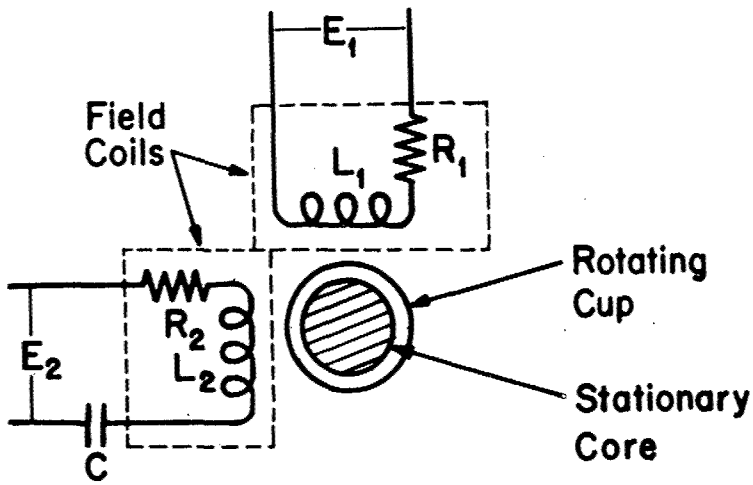

Figure 18. Electrical components in a drag cup motor

with

$$a = 0 \quad \text{for } \kappa < \kappa_c$$

$$a = 0.8 \text{ for } \kappa \geq \kappa_c$$

Thus, for a given material the shear stress increases linearly with increasing κ to some value $\sigma_c = \eta_0 \kappa_c$, then increases only very slowly according to

$$\sigma \cong \sigma_c (\kappa/\kappa_c)^{0.2}$$

for further increase in κ. An estimate for σ_c is possible using the correlations for $\eta(\kappa)$ described in a previous report[2]

$$\eta(\kappa) = \eta(0) Q(\kappa/\kappa_0)$$

where the function $Q(\kappa/\kappa_0)$ is independent of molecular weight, and κ_0 is a reducing parameter roughly equal to the rate of shear at which $\eta(\kappa)$ begins to decrease with increasing κ. The product

$$J_\eta^{-1} \equiv \kappa_0 \eta_0 = \sigma_0$$

tends to be independent of M for M greater than the critical molecular weight M_c for which η changes from proportionality with M to proportionality with $M^{3.4}$. Moreover, J_η appears to be of the same order of magnitude as the equilibrium compliance J_e,[2] with values of the order 10^{-6} cm^2/dyne or greater, for undiluted polymers, increasing as φ_2^{-2} on dilution. Thus, the value of σ_c can be predicted to be of the order 10^6 dyne/cm^2 for concentrated solutions as rough estimates. Therefore, we do not anticipate any difficulty in torque requirements when working with concentrated solutions of BBB. A cone and plate slightly smaller than the 2 cm radius assembly might have to be utilized for any future work with melts of an undiluted polymer, however, or could be used with concentrated solutions of BBB if torque requirements exceeded the output of the drag cup motor.

Equation (42) can be used to calculate the optimum circuit parameters for maximum torque output. Setting (cf. Fig. 18)

$$i_1 = E_1 Z_1^{-1} = E_1 [R_1^2 + X_{L1}^2]^{-\frac{1}{2}}$$

$$i_2 = E_2 Z_2^{-1} = E_2 [R_2^2 + (X_{L2} - X_c)^2]^{-\frac{1}{2}} ,$$

and

$$\sin \theta_{12} = \sin \left\{ \arctan \left(\frac{X_{L2} - X_c}{R_2} \right) - \arctan \left(\frac{X_{L1}}{R_1} \right) \right\} ,$$

the value of the external capacitance impedence X_c for maximum torque at a given voltage E_1 and E_2 can be computed from

$$\left(\frac{\partial T}{\partial X_c} \right)_{E_1, E_2} = 0$$

to give the transendental relation

$$\arctan \left(\frac{X_{L2} - X_c}{R_c} \right) - \arctan \left(\frac{X_{L1}}{R_1} \right) = \arctan \left(\frac{R_2}{X_{L2} - X_c} \right)$$

that must be solved by trial and error methods. The internal impedences X_{L1}, X_{L2}, R_1, and R_2 must be measured in separate experiments in order to calculate sin θ_{12}.

Equation (42) also reveals the source of an observed dependence on temperature for the torque produced by the drag cup motor. Relatively small variation in the impedence of the components can cause appreciable variation in, for example, sin θ_{12}, resulting in a larger variation on T. For this reason, the drag cup motor must be held at constant temperature. This can be accomplished by circulating a thermostated liquid through a heat exchanger in contact with the field coils.

V. Dilute Solution Studies on a Polyphenylene Polymer —— G. C. Berry and S. M. Liwak

A polyphenylene polymer GN-121 with the idealized structure

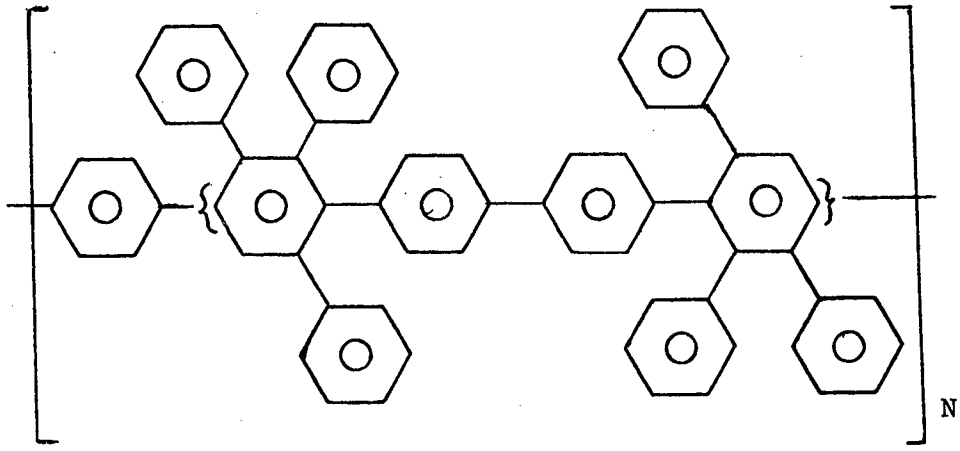

was provided by Dr. J. Stille of the University of Iowa. The polymer was originally presumed to contain all <u>para</u> links, producing a molecule with a rodlike conformation, but later work by Dr. Stille on model reactions suggests the possibility of some <u>meta</u> groups in the positions shown (the extent of this isomerization is unknown, but should be less than about 20% according to model reactions). Fractionation and dilute solution studies were undertaken on GN-121 before this complication was appreciated, in the hope that this polymer would provide a suitable model for the study of the solution and bulk properties of rodlike chains. The results indicate that the fractions may approach a rod conformation at low molecular weight, but that appreciable branching is present in the higher molecular weight fractions. This study does not represent a complete analysis of the properties of the GN-121 polymer, but investigation was halted when the polymers were found not to be completely rodlike.

1. <u>Solubility and Fractionation</u>.

The polymer as received was soluble in a number of organic solvents including toluene, chloroform and tetrahydrofuran (THF). Some of the preliminary solubility and fractionation studies were carried out on a small amount of polymer GN-91, which had a slightly greater M_n than GN-121. It was discovered that unfractionated polymer coagulated slowly from a toluene-methanol mixture would not redissolve in toluene. The polymer so treated was soluble in chloroform, and was, moreover, soluble in toluene after recovery from chloroform solution by evaporation. Wide angle x-ray scattering

revealed a diffuse 7.0 A spacing in the untreated polymer that became sharper for the toluene insoluble polymer. The tendency to form toluene material was noticeably greater for the fractions. Presumably, this tendency to form a toluene insoluble material is related to the formation of ordered regions in the polymer, reflecting the tendency to form parallel arrangements of the chains. The development of ordered regions would be expected to be enhanced by a fractionation that removed short chain length species. The 7.0 A spacing is interpreted as the radial separation of the rodlike chains in the parallel arrays.

The fractionation of GN-121 was carried out from a 0.1% solution in a chloroform-methanol mixture at 25°C by the successive addition of methanol to remove the fractions. No difficulty was encountered in the redissolution of the polymer at elevated temperatures (40°C) after addition of methanol to reach the cloud point. The fractions were analyzed on a calibrated Waters Gel Permeation Chromatograph so that values of $[\eta]M$ were assigned to the maximum elution volume. The breadth of the elution curves was consistent with that to be expected for good fractions, with the exception of fractions numbers 5 and 6 out of a total of 21 fractions. The failure of these fractions to conform to the overall pattern is not understood, but probably reflects some loss of control of the operating parameters in the fractionation system. The values of $[\eta]M$ obtained from the maximum elution volume will be discussed below.

Curves for the cumulative weight fraction versus the molecular weight were constructed for the whole polymer from the fractionation data and from the elution profile for the unfractionated polymer (uncorrected for diffusion spreading). Both curves showed the presence of a very long, high molecular weight tail comprising less than ca. 10 percent of the total polymer. These species are contained in the first 4 to 5 fractions of the fractionated polymer. Values of M_w and M_n from the fractionation data were 16.4×10^4 and 3.39×10^4, respectively, indicating a distribution far more disperse than that for a usual condensation polymer. Calculation of M_w for the data excluding the first three fractions yields a value of 6.5×10^4 (with M_n unaffected).

2. Intrinsic Viscosity

Intrinsic viscosities were obtained in suspended Ubhellode viscometers at 25°C. Viscosities were determined in one, or more, of the solvents THF, chloroform, or toluene. The data, listed in Table VIII reveal no appreciable solvent effect on the value of $[\eta]$.

TABLE VIII

Intrinsic Viscosity of Fractions of Polyphenylene Polymer GN-121 in Several Solvents at 25°C

Fraction	[η] Tetrahydrofuran	Chloroform	Toluene
1	3.11	---	---
3	1.60	1.60	---
5	---	1.48	---
7	1.13	---	---
8	1.18	---	---
9	0.98	0.95	0.93
10	---	0.57	---
12	0.57	---	---
14	---	0.37	---
16	---	---	0.35

3. Osmotic Pressure

The osmotic pressure of dilute solutions was measured with a Mechrolab Model 501 osmometer using Schleicher and Schuell number 0-8 membranes. Data were taken in tetrahydrofuran, toluene, or chloroform. The data were not altogether satisfactory in reproducibility. The reason for the difficulty is not certain; but it is suspected that complete solubility may not always have been achieved. The values of M_n recorded in Table IX are certainly no better than ± 10 per cent.

4. Exclusion Chromatography

The maximum elution volume V_e of each of the fractions in tetrahydrofuran was used to compute $[\eta]M$ from a correlation of $[\eta]M$ versus V_e obtained for polystyrene fractions. Values of M_{GPC} calculated from $[\eta]M$ and the observed value of $[\eta]$ in tetrahydrofuran are given in Table IX. It is of interest that the values of M_{GPC}, M_w and M_n are in reasonable agreement, despite the departure of GN-121 from the random coil conformation of the calibration polymer polystyrene. The agreement is certainly good enough to allow the use of M_{GPC} as a molecular weight measure for these fractions.

5. Light Scattering

Light scattering experiments were carried out on the Mellon Institute instrument using the standard cell and the green Hg line, with the exception of the measurements on fraction 1 for which the small centrifugable light scattering cell was used. Solutions for the standard cells were clarified by filtration through 0.45 micron membrane filters. Fraction 1 could not be filtered in this way since it repeatedly clogged the membrane filters. Fraction 2 clogged the filter on the first pass, but could be filtered on a new membrane afterwards. Some much less severe slowing of the filtration rate was noted with fraction 3, but the remaining fractions were filtered without difficulty.

No outstanding difficulties were encountered other than the filtration of the high molecular weight fractions. Depolarization of the scattering was checked and found to be negligible. The solutions were not absorbing for the green light, although they would have been for blue light. The data on the mean-square radius of gyration $\langle s^2 \rangle$, M_w and the second virial coefficient Γ_2 are collected in Table X.

6. Discussion

The long, high molecular weight tail found in GN-121, together with the filtration difficulties encountered with the high

TABLE IX

Molecular Weight of Fractions of GN-121 by Light Scattering, Osmometry and Exclusion Chromatography

Fraction	$10^4 M_w$	$10^4 M_n$	$10^4 M_{GPC}$
1	182	---	170
3	51	---	48
7	21	29	24
8	13	---	15
9	7.8	7.8	7.6
12	---	3.0	3.5
14	---	2.1	1.8
16	---	2.7	1.5

TABLE X

Light Scattering Data on Fractions of GN-121 in Tetrahydrofuran

Fraction	$10^4 M_w$	$10^{12} \langle s^2 \rangle$ (cm^2)	$10^{12} \langle s^2 \rangle_{ROD}^*$	Γ_2 (cc/g)
1	182	84.3	17.4×10^3	396
2	78.0	36.3	3.20	90
3	50.8	14.2	1.36	172
7	20.7	12.2	0.26	53
8	12.7	4.4	0.085	68
9	7.8	2.0	0.032	97

*Calculated for a perfect rod conformation at the given value of M.

molecular weight fractions, suggests that branching and subsequent gel formation may have occurred in the polymerization. This conclusion is strengthened by the data on log $[\eta]$ versus log M shown in Figure 19. The intrinsic viscosity for a very long rodlike molecule of length L and diameter a should obey the relation

$$[\eta]_{ROD} = (8.4 \times 10^{20}) \frac{L^2 a}{M_0 \ln(L/a)}$$

where

$$L = \frac{Ma}{M_0}$$

or

$$[\eta]_{ROD} = (8.4 \times 10^{20}) \left(\frac{a}{M_0}\right)^3 \frac{M^2}{\ln(M/M_0)}$$

$$[\eta]_{ROD} = \frac{40.4 \times 10^{21}}{\ln(L/a)} \frac{\langle s^2 \rangle_{ROD}^{3/2}}{M}$$

The final representation for $[\eta]$ uses the relation

$$\langle s^2 \rangle_{ROD} = \frac{1}{12} L^2 \quad ,$$

and illustrates the interesting result that the product $[\eta]M\langle s^2\rangle^{-3/2}$ takes on a value nearly independent of M for large M, as it does for coils (e.g., if $L/a \sim 10^3$, then $[\eta]M\langle s^2\rangle^{-3/2} \simeq 6 \times 10^{21}$). Setting M_0 equal to a value such that the distance along the chain is equal to 8 Å, which is taken as the chain diameter, we get the curve shown in Figure 19 for these polyphenylene polymers. The calculated $[\eta]_{ROD}$ deviates markedly from the observed values increasingly as M increases. This behavior could reflect 1) increased intrachain flexibility as M increases owing to the meta imperfections described above, or 2) increased chain branching with increasing M.

Unfortunately, it does not appear possible to distinguish neatly between these two alternatives solely on the basis of the dilute solution data in hand. Thus, if we assume that all of the possible placements were taken up by meta links, $[\eta]$ can be reasonably calculated from the value of $\langle s^2 \rangle$ for the freely rotating chain and the relation for $[\eta]$ for a random coil (the presence of the unsubstituted phenylene para links would be expected to render such a chain freely rotating). Using the freely rotating chain model, for which

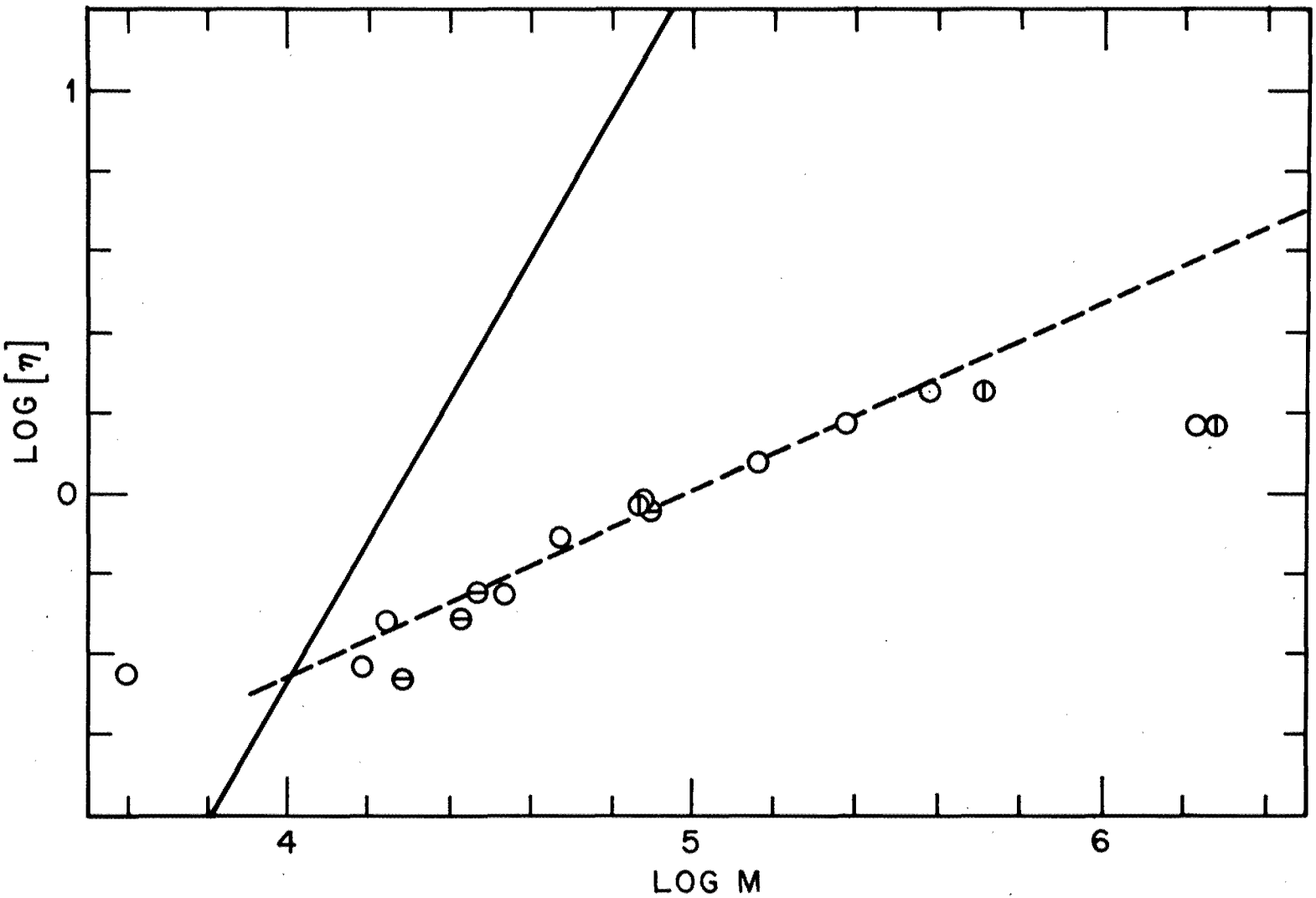

Figure 19. Log [η] versus log M for polymer GN-121 tetrahydrofuran. Values of M from light scattering, ⊖; osmometry, ◐; or exclusion chromatography ○. The solid line represents the expected behavior for rod molecules. The empirical dashed line has slope 0.47

$$\langle s^2 \rangle_{COIL} = \frac{1}{6} Nb^2 \frac{1 + \cos \alpha}{1 - \cos \alpha} ,$$

values of $\langle s^2 \rangle_{COIL}$ can be estimated with N = M/418, b = 10.5 A and the supplementary bond angle $\alpha = 60°$. Thus for $M = 4.18 \times 10^5$, we calculate $\langle s^2 \rangle_{COIL} = 5.5 \times 10^{-12}$ cm^2 and $[\eta]_{COIL} = 1.2$ dℓ/g compared to the values of $\langle s^2 \rangle = 16 \times 10^{-12}$ cm^2 and $[\eta] = 1.8$ interpolated for this M from the observed values. This seems to indicate that a much greater percentage of the placements would have to be meta than the maximum 20 per cent suggested by Dr. Stille if this effect alone is envoked to explain the observed values of $\langle s^2 \rangle$ and $[\eta]$.

Another model can be envoked supposing that the actual configuration is compressed of rodlike chain segments in a branched array. The radius can be calculated from

$$\langle s^2 \rangle = \frac{b^2}{n^2} \sum_{i,j} \sum \langle L_{ij}^2 \rangle$$

if it is assumed for simplicity that the branched configuration is starlike. This should give the maximum decrease in $\langle s^2 \rangle$ for a given number of branches. With this approximation,

$$g_{ROD} = \frac{\langle s^2 \rangle_{br}}{\langle s^2 \rangle_{\ell}} = \frac{1}{f^3}$$

for f rodlike chains freely jointed at the center; $\langle s^2 \rangle_{\ell}$ is the radius of the linear rodlike chain of the same mass as the line on chain. The calculated values of g_{ROD} from the data in Table X range from 0.005 to 0.06, compared to the values 0.0156 and 0.0385 for f equal to 4 and 3, respectively. Thus, the observed values of $\langle s^2 \rangle$ could reflect mainly branching, with little or no meta placements and consequent intrachain flexibility.

We are inclined to believe that there is considerable branching in the polymer studied for several reasons:

1. the apparent gel fraction found at high molecular weights,

2. the molecular weight distribution skewed toward high M, and

3. the extremely high meta content required to explain the values of $\langle s^2 \rangle$ and $[\eta]$ observed.

This does not, however, rule out the possibility that the suspected branching is accompanied by up to 20 per cent meta placements. As stated earlier, the investigation was terminated at the present inconclusive stage since whatever the actual configuration, it is evidently not a linear rodlike chain molecule.

REFERENCES

1. G. C. Berry and S.-P. S. Yen, Adv. Chem. Series, in press.

2. Technical Report AFML-TR-67-92, Pt. III, January 1969.

3. E. L. Wehry, in Fluorescence, edited by G. G. Guilbault, Chapter 2, Marcel Dekker, Inc., (1967), New York.

4. H. C. van de Hulst, Light Scattering by Small Particles, p. 85ff, John Wiley & Sons, Inc., New York (1957).

5. G. C. Berry and E. F. Casassa, Macromolecular Reviews, Vol. 4, in press.

6. E. F. Casassa and H. Eisenberg, Adv. Protein Chim. 19, 287 (1964).

7. A. R. Glascow, N. C. Krouskop and F. D. Rossini, Anal. Chem. 22, 1521 (1950).

8. W. J. Taylor and F. D. Rossini, J. Research, Natl. Bur. Stds. 32, 197 (1944).

9. R. J. Gillespie and E. A. Robinson in Non-Aqueous Solvent Systems, ed. by T. C. Waddington, Chapter 4, Academic Press, New York (1965).

10. S. J. Bass, R. J. Gillespie and E. A. Robinson, J. Chem. Soc., 814 (1960).

11. ASD Technical Report 61-22, p. 71.

12. G. C. Berry and T. G Fox, Adv. Polymer Sci., 5, 262 (1968).

13. Technical Report AFML TR-67-92, p. 164.

14. A. H. Bloksma, Rheologica Acta 2, 217 (1962).

15. D. J. Plazek, J. Polymer Sci., Part A-2, 6, 621 (1968).

16. M. H. Birnboim, private communication.

17. H. Markovitz, L. J. Elyash, F. J. Padden, and T. W. DeWitt, J. Colloid Sci. 10, 165 (1955).

18. Tube Laboratory Manual, Mass. Inst. Tech. Res. Lab. of Electronics, Second Ed., p. 2, 11, 18, Cambridge, Mass. (1956).

19. S. A. Davis and B. K. Ledgerwood, Electromechanical Components for Servomechanisms, McGraw-Hill, New York (1961).

UNCLASSIFIED
Security Classification

DOCUMENT CONTROL DATA - R & D

(Security classification of title, body of abstract and indexing annotation must be entered when the overall report is classified)

1. ORIGINATING ACTIVITY *(Corporate author)*
Mellon Institute
Carnegie-Mellon University
4400 Fifth Avenue
Pittsburgh, Pa. 15213

2a. REPORT SECURITY CLASSIFICATION
UNCLASSIFIED

2b. GROUP

3. REPORT TITLE
POLYMER STRUCTURES AND PROPERTIES

4. DESCRIPTIVE NOTES *(Type of report and inclusive dates)*
Technical Documentary Report, (February 1, 1969 to January 31, 1970)

5. AUTHOR(S) *(First name, middle initial, last name)*
G. C. Berry, J. S. Burke, E. F. Casassa, S. M. Liwak

6. REPORT DATE	7a. TOTAL NO. OF PAGES	7b. NO. OF REFS
January 1970	75	19

8a. CONTRACT OR GRANT NO.	9a. ORIGINATOR'S REPORT NUMBER(S)
F33615-69-C-1268	
b. PROJECT NO. 7340	
c. Task No. 734004	9b. OTHER REPORT NO(S) *(Any other numbers that may be assigned this report)*
d.	

10. DISTRIBUTION STATEMENT This document is subject to special export controls and each transmittal to foreign governments or foreign nationals may be made only with prior approval of the Nonmetallic Materials Division (MANP), Air Force Materials Laboratory, Wright-Patterson Air Force Base, Ohio 45433.

11. SUPPLEMENTARY NOTES	12. SPONSORING MILITARY ACTIVITY
	Nonmetallic Materials Division, Air Force Materials Laboratory, Air Force Systems Command, Wright-Patterson AFB, Ohio

13. ABSTRACT

Experimental studies on the heterocyclic polymer BBB, obtained by the condensation reaction of 3,3'diaminobenzidine with naphthalene-1,4,5,8-tetracarboxylic acid, are described. Fractionations based on exclusion chromatography and selective solubility are discussed. Dilute solution properties of these fractions including light scattering and viscometry are presented.

The viscosity of concentrated solutions of the fractions in methane sulfonic acid is studied as a function of concentration and molecular weight of the polymer, and temperature. It is concluded that the solutions have a high entanglement density, even at relatively low polymer concentration, and that the segmental friction factor increases very fast with increasing polymer concentration. The latter effect is probably associated with the inability to form homogeneous solutions of BBB at high concentration.

Freezing temperature studies on solutions of a model compound of the BBB repeat unit are described. These show the compound to be diprotonated in sulphuric acid.

The design of a cone and plate viscometer for rheological studies on BBB solutions is discussed.

Dilute solution properties on a candidate 'rod-like' polymer are presented. These show that the anticipated rod-like character of the polymer is only imperfectly realized.

DD FORM 1 NOV 65 1473

UNCLASSIFIED
Security Classification

14. KEY WORDS	LINK A		LINK B		LINK C	
	ROLE	WT	ROLE	WT	ROLE	WT
Organic Chemistry						
Polymers, Statistics						
Polymers, Structure						
Polymers, Heterocyclic						
Thermodynamics						
Light Scattering						
Viscosity						
Chromatography						
Gel Permeation						
Freezing Temperature						